VINÍCIUS ANDRADE MAIA

DINÂMICA DO CARBONO EM FLORESTAS TROPICAIS BRASILEIRAS EXTRA-AMAZÔNICAS

LAVRAS – MG
2021

VINÍCIUS ANDRADE MAIA

DINÂMICA DO CARBONO EM FLORESTAS TROPICAIS BRASILEIRAS EXTRA-AMAZÔNICAS

Dissertação apresentada à Universidade Federal de Lavras, como parte das exigências do Programa de Pós-Graduação em Engenharia Florestal, área de concentração em Ecologia Florestal, para a obtenção do título de Mestre.

Dr. Rubens Manoel Dos Santos

Orientador

LAVRAS – MG

2021

Ficha catalográfica elaborada pelo Sistema de Geração de Ficha Catalográfica da Biblioteca Universitária da UFLA, com dados informados pelo(a) próprio(a) autor(a).

Maia, Vinícius Andrade.
Dinâmica do carbono emflorestas tropicais brasileiras extra-amazônicas / Vinícius Andrade Maia. - 2021.
77 p.

Orientador(a): Rubens Manoel dos Santos.

Dissertação (mestrado acadêmico) - Universidade Federal de Lavras, 2021.
Bibliografia.

1. Sumidouro de carbono florestal. 2. Estoques de carbono. 3. Mudanças climáticas. I. Santos, Rubens Manoel dos. II. Título.

VINÍCIUS ANDRADE MAIA

DINÂMICA DO CARBONO EM FLORESTAS TROPICAIS BRASILEIRAS EXTRA-AMAZÔNICAS

CARBON DYNAMICS IN EXTRA-AMAZON TROPICAL FORESTS IN BRAZIL

Dissertação apresentada à Universidade Federal de Lavras, como parte das exigências do Programa de Pós-Graduação em Engenharia Florestal, área de concentração em Ecologia Florestal, para a obtenção do título de Mestre.

APROVADA em 26 de março de 2021.
Dr. Jean Daniel Morel – UFLA
Dr. Fernanda Coelho de Souza – UNB
Dr. Jamir Afonso do Prado Júnior - UFU

Prof. Dr. Rubens Manoel dos Santos
Orientador

LAVRAS – MG
2021

AGRADECIMENTOS

Primeiramente agradeço à minha mãe, Walmira, por tudo, e também à todas as pessoas queridas que me rodeiam e estão comigo. Agradeço também ao meu orientador Rubens Santos, pelo conhecimento partilhado, orientação, entusiasmo e oportunidades. Agradeço ao companheirismo de todos os amigos e amigas do Laboratório de Fitogeografia e Ecologia Evolutiva. Agradeço a todos os funcionários e professores da Universidade Federal de Lavras que contribuem diretamente e indiretamente com o desenvolvimento da ciência e formação dos estudantes.

Agradeço as universidades públicas, e em especial a Universidade Federal de Lavras, pelo papel importante que desempenham na sociedade. Agradeço às políticas e financiamentos governamentais, bem como CAPES, CNPq e FAPEMIG, que permitem o desenvolvimento da ciência no país, e que possibilitaram que eu e muitas pessoas tenham tido todas essas oportunidades.

Agradeço por todas as oportunidades e ajudas que recebi e espero que esse trabalho contribua para um mundo melhor, e que seja uma oportunidade para retribuir os privilégios que possuo.

RESUMO

O funcionamento do sistema terrestre vem sendo alterado de maneira drástica devido às mudanças climáticas provocadas por atividades humanas. Dessa maneira, a necessidade de entender as respostas dos ecossistemas para que se possa predizer o comportamento futuro vem sendo cada vez maior e urgente. No componente terrestre, as florestas realizam diversas funções ecossistêmicas, dentre elas a produtividade primária e a ciclagem do carbono. Essas funções têm sido afetadas pelos efeitos das mudanças climáticas e aumentos das emissões de CO_2, de maneira que a provisão desses serviços ecossistêmicos pode estar comprometida nas próximas décadas. Essas alterações afetam toda a dinâmica do planeta, e, portanto, a sobrevivência das espécies e a qualidade de vida da espécie humana. O objetivo desse estudo foi entender os padrões espaciais e temporais de estoque e estocagem de carbono em florestas tropicais no sudeste do Brasil. Esses resultados visam contribuir para a construção do conhecimento em relação a funcionalidade de florestas tropicais e seus biomas, bem como auxiliar tomadas de decisão em relação a políticas ambientais de proteção e conservação da biota terrestre.

Palavras-chave: Sumidouro de carbono florestal. Estoques de carbono. Mudanças climáticas.

ABSTRACT

The Earth's ecosystem functioning has been dramatically altered by climate change and human activities over the recent decades. Therefore, it is urgent to understand the ecosystems responses to these changes. In the earth system, forests play an important role in many ecosystem functions, among them the primary net productivity and carbon cycling. However, these functions have been affected by changes in climate and increasing CO_2 emissions, in a way that the provision of these ecosystem services may be compromised in the next decades. These changes may affect the whole planet dynamics, and therefore species survival and human well-being. The aim of this study was to understand the spatial and temporal patterns of carbon stocks and sinks of tropical forests in southeastern Brazil. These results contribute to knowledge of the functionality of tropical forests and its biomes and assist in conservation policies and decision making to protect the terrestrial biota.

Keywords: Forest carbon sink. Carbon stocks. Climate change.

SUMÁRIO

PRIMEIRA PARTE

1 INTRODUÇÃO

As florestas tropicais cobrem 10% da superfície do planeta e estocam cerca 50% do carbono terrestre, sendo responsáveis por um terço da produtividade primária líquida, além de abrigarem uma grande parte da biodiversidade (CORLETT, 2016; PAN et al., 2011). As formações florestais são cruciais para a ciclagem do carbono na Terra e interagem com outros ciclos, como os ciclos dos nutrientes e o hidrológico (CORLETT, 2016; PAN et al., 2011). No entanto, devido as ações antrópicas, principalmente desde a revolução industrial, o clima vem sendo alterado, com diversos efeitos na biosfera e na provisão de serviços ecossistêmicos (LEWIS, 2006; ROBERTS; BOIVIN; KAPLAN, 2018). As mudanças climáticas ameaçam o sumidouro de carbono terrestre, o que pode agravar ainda mais as alterações climáticas, já que as florestas afetam e são afetadas pelo clima (CORLETT, 2016). Além dos aumentos nos eventos de seca e temperatura relacionados aos aumentos na concentração de CO_2 na atmosfera, espera-se aumentos nas ocorrências de fogo e desmatamento nas próximas décadas, o que pode fazer com que as florestas tropicais deixem de ser sumidouros e se tornem fontes de carbono (BACCINI et al., 2017; CORLETT, 2016; HUBAU et al., 2020; MAGRIN et al., 2014).

Os efeitos de precipitação e temperatura nos estoques de carbono florestais se devem, principalmente, às respostas ecofisiológicas dos vegetais às variáveis ambientais (ÁLVAREZ-DÁVILA et al., 2017; MCDOWELL et al., 2018; TAYLOR et al., 2017). O principal processo da produtividade primária é a fotossíntese, que depende da concentração de dióxido de carbono, de uma faixa ótima de temperatura e da água, que é o solvente necessário para as principais reações químicas essenciais ao metabolismo (BOISVENUE; RUNNING, 2006; HOPKINS; HÜNER, 2004). Portanto, as alterações climáticas afetam diretamente o metabolismo vegetal, refletindo em aspectos mais amplos, como a ciclagem do carbono em nível de ecossistema (PAN et al., 2011). A mortalidade de árvores, componente crucial da produtividade florestal, é altamente afetada por condições ambientais, onde aumentos de temperatura e eventos de seca, que além de diminuírem as taxas de crescimento (fotossíntese), levam à mortalidade devido à falha hidráulica e aumentos nas taxas de respiração, afetando negativamente a produtividade primária (MCDOWELL et al., 2018). O aumento nas concentrações de CO_2 atmosférico, conhecido como fertilização da atmosfera, teoricamente deveria aumentar as taxas de crescimento já que CO_2 é essencial para a realização da fotossíntese, . Dessa maneira, embora o aumento nas concentrações de CO_2 atmosférico aumente a temperatura do planeta, devido ao incremento do efeito estufa, o aumento nas taxas de fotossíntese provocado pelo aumento da

concentração de CO_2 seria maior que o aumento nas taxas de respiração provocado pelo aumento da temperatura. Além de temperatura e precipitação, os nutrientes, como fósforo e nitrogênio, são cruciais para a produtividade primária, já que constituem moléculas importantes para o metabolismo vegetal (CLEVELAND et al., 2011; NORBY et al., 2010; TURNER; BRENES-ARGUEDAS; CONDIT, 2018). Sendo assim, em síntese, os estoques de carbono e produtividade são altamente relacionados às variáveis climáticas e edáficas.

Os efeitos das alterações climáticas não se restringem apenas aos individuos e comunidades, alcançando níveis de maior escala, como biomas e ecossistemas (MITCHARD, 2018; PAN et al., 2013). O conjunto das respostas das comunidades locais podem ocasionar a formação de biomas e ecossistemas funcionalmente distintos dos atuais devido a tolerância e adaptação das espécies à certas condições e recursos (ARRUDA et al., 2017a; MCELWAIN, 2018; PAN et al., 2013; PENNINGTON; LAVIN; OLIVEIRA-FILHO, 2009). As mudanças climáticas, além de selecionarem espécies aptas às novas condições ambientais, podem gerar novos padrões de funcionamento, onde alguns biomas atuais podem convergir para um comportamento semelhante, ou divergir para comportamentos distintos (MCELWAIN, 2018). Portanto, é importante entender como as florestas de diferentes biomas têm respondido às mudanças ambientais ao longo do tempo. A partir desse entendimento será possível predizer o estoque e sumidouro de carbono de maneira detalhada e específica para cada tipo de floresta, fundamentando e orientando tomadas de decisão nos âmbitos ecológico e político (ARRUDA et al., 2017a; CORLETT, 2016; GAZOL et al., 2018; MCDOWELL et al., 2018; MCELWAIN, 2018; PAN et al., 2011, 2013).

2 REFERENCIAL TEÓRICO

2.1 O sistema terrestre, serviços ecossistêmicos e o carbono

O carbono é um elemento chave para o sistema terrestre e para a vida na Terra, devido ao seu papel em todas as camadas e, especialmente, no metabolismo de todos os organismos vivos (MITCHARD, 2018; ZUMDAHL; ZUMDAHL; DECOSTE, 2017). Ao longo do ciclo do carbono, esse elemento flui entre a atmosfera e a superfície, através dos seres vivos, solo e oceanos, sendo que alguns processos estão compreendidos em escala de décadas e outros em milhares de anos, como o carbono mineralizado (ARCHER, 2010; ZUMDAHL; ZUMDAHL; DECOSTE, 2017). A fotossíntese está entre um dos processos mais importantes do sistema terrestre por ser o processo por onde a energia vinda do Sol entra no sistema do planeta Terra (LI et al., 2018). A partir do processo de fotossíntese, a energia começa a fluir pelo sistema, desde a produtividade primária até o final da rede trófica, sendo, portanto, um processo chave para o funcionamento do sistema terrestre e para a vida (ARCHER, 2010; LI et al., 2018). O fluxo do carbono ocorre através de um conjunto de processos, como a fotossíntese, respiração, decomposição e mineralização. O ciclo do carbono é altamente interconectado com os outros ciclos essenciais para o planeta, como o ciclo do oxigênio, ciclo do nitrogênio e ciclo hidrológico. Esses ciclos (e outros não mencionados) interagem para determinar a produtividade primária, padrões climáticos, suprimento de água e diversos outros serviços ecossistêmicos (LE QUÉRÉ et al., 2018; MITCHARD, 2018).

No último século a população humana alcançou a casa dos bilhões, e as influências humanas sobre o ambiente atingiram níveis críticos (ROBERTS; BOIVIN; KAPLAN, 2018). A dinâmica do sistema terrestre, especialmente o ciclo do carbono, vem sendo alterada principalmente devido à queima de combustíveis fósseis desde a revolução industrial no século XVIII. Juntamente com a queima de combustíveis fósseis, houve aumento significativo nas mudanças no uso da terra e no desmatamento, afetando de maneira crítica a ciclagem do carbono (KEENAN et al., 2015; KEENAN; WILLIAMS, 2018; LE QUÉRÉ et al., 2018; MITCHARD, 2018). Essas mudanças estão provocando aumentos no CO_2 atmosférico, indo de 277 ppm para 409 desde o começo da revolução industrial (1750) até 2018, sendo principalmente por mudanças no uso da terra até 1950, e a partir disso devido a queima de combustíveis fósseis (DLUGOKENCKY; TANS, 2019; LE QUÉRÉ et al., 2018). Desde a década de 60 as emissões de CO_2 aumentaram drasticamente, indo de 3,1 Gt C ano^{-1} na década

de 1960 para 9,4 Gt C ano^{-1} entre 2008-2017 (LE QUÉRÉ et al., 2018). As emissões são particionadas nos sumidouros da atmosfera, oceano e terrestre, os quais também aumentaram seus estoques de CO_2 desde a década de 1960, de 1,7 Gt C ano^{-1} para 4,7 Gt C ano^{-1} na atmosfera, de 1 Gt C ano^{-1} para 2,4 Gt C ano^{-1} nos oceanos; e de 1,2 Gt C ano^{-1} para $3,2 \pm 0,7$ Gt C ano^{-1} no sumidouro terrestre, sendo, respectivamente 47,9%, 25,5% e 34.1% do total de emissões (LE QUÉRÉ et al., 2018).

O CO_2 atmosférico intercepta a radiação refletida pela superfície, de maneira que parte do calor fica retida na atmosfera e outra parte é difundida para o espaço. Esse efeito, conhecido como efeito estufa, é um efeito natural e fundamental para a manutenção do clima e da vida no planeta, sendo um importante serviço ecossistêmico em nível global (LE QUÉRÉ et al., 2018). O aumento das emissões e das concentrações de CO_2 na atmosfera intensifica esse processo, de maneira que mais calor fique retido na atmosfera, aumentando a temperatura do planeta KEENAN; WILLIAMS, 2018; PACHAURI; MEYER, 2014). Esse aumento de temperatura global afeta os seres vivos de maneira ampla, alterando as suas relações entre si e com o ambiente (MCDOWELL et al., 2018). As mudanças climáticas também estão relacionadas a alterações no regime de secas, com mudanças na intensidade, frequência e duração desses eventos (PACHAURI; MEYER, 2014). Essas mudanças afetam toda a dinâmica do sistema terrestre, especialmente a biosfera, bem como diversas atividades produtivas, industriais e agrícolas, comprometendo diretamente a qualidade de vida humana, a economia e a sociedade (KEENAN; WILLIAMS, 2018; LE QUÉRÉ et al., 2018).

As atividades humanas e seus impactos no ambiente, estão atingindo um ponto crítico, o que motivou diversos pesquisadores a considerar o momento atual como um período distinto, o antropoceno (ROBERTS; BOIVIN; KAPLAN, 2018). O antropoceno está associado ao impacto das atividades humanas, que devido a sua intensidade e abrangência determinam padrões exclusivos, que seriam impossíveis na natureza sem as atividades humanas (ROBERTS; BOIVIN; KAPLAN, 2018). Na zona terrestre, pode-se destacar o papel desempenhado pelas florestas, que são os principais sumidouros de carbono (MITCHARD, 2018; PAN et al., 2013). O sequestro de carbono realizado pela fotossíntese constitui um importante serviço ecossistêmico realizado pelas florestas, que a partir da produtividade primária provém energia para os demais componentes do sistema e controlam o clima do planeta. No entanto, o crescente desmatamento, queimadas, mudanças climáticas e outros distúrbios, podem fazer com que as florestas deixem de ser um sumidouro de carbono e se tornem fontes de carbono nas próximas décadas (HUBAU et al., 2020; PAN et al., 2011).

Em nível global, estima-se que 75% da produtividade primária bruta terrestre e 80% da biomassa total esteja na cobertura florestal, sendo as florestas tropicais as de maior estoque e produtividade (262,1 Pg C, 2,41 Pg C/ano, respectivamente), seguidas pelas florestas boreais (53,9 Pg C, 0.5 Pg C/ano) e florestas temperadas (46,6 Pg C, 0.72 Pg C/ano) (MITCHARD, 2018; PAN et al., 2011, 2013). No entanto, esses números podem mudar nas próximas décadas devido às mudanças climáticas, que influenciam a vegetação, de maneira que a produtividade seja alterada devido ao aumento na frequência e intensidade de eventos de seca e variações na temperatura. Essas alterações possuem diversos impactos não só no ciclo do carbono, mas também na ciclagem de nutrientes e no ciclo hidrológico, com alterações no regime de chuvas e impactos relevantes nas atividades agrícolas e na provisão de alimentos. Como as florestas afetam e são afetadas pelo clima, as mudanças climáticas podem gerar um efeito cascata, e a perda florestal proveniente do desmatamento seria um fator agravante.

2.2 Estoques e estocagem de carbono em florestais tropicais

Embora a atividade biológica das plantas seja altamente dependente da radiação solar, outros fatores também são de grande importância para os processos fotossintéticos. Dentre esses fatores, pode-se citar o dióxido de carbono na atmosfera, disponibilidade de água, temperatura e nutrientes disponíveis no solo (BOISVENUE; RUNNING, 2006). Portanto, atributos relacionados aos fatores climáticos, edáficos e suas interações, são de grande importância para compreender os processes que condicionam a produtividade vegetal. As respostas fisiológicas das plantas às condições ambientais, são, portanto, muito relacionadas aos filtros ambientais nos quais o local está submetido no espaço e no tempo (MALHI, 2012; MCDOWELL et al., 2018).

Aumentos de temperatura, por exemplo, podem condicionar aumentos no déficit de pressão de vapor no ar, aumentando as taxas de transpiração, o que é um efeito adverso e afeta negativamente a produtividade devido à perda de água (BOISVENUE; RUNNING, 2006; CORLETT, 2016; MALHI, 2012). O metabolismo vegetal é em grande parte influenciado pela temperatura, o que determina a capacidade fotossintética e a produtividade, sendo a faixa ótima de temperatura para a produtividade compreendida entre 15-25ºC (BOISVENUE; RUNNING, 2006; HOPKINS; HÜNER, 2004). No entanto, evidências recentes indicam que os estoques de carbono das florestas tropicas úmidas podem ser resilientes caso a temperatura máxima se mantenha abaixo de 32.2 ºC (SULLIVAN et al., 2020). A água, por sua vez, é o principal

componente celular, sendo um solvente universal, que permite a ocorrência de reações químicas necessárias para o metabolismo dos seres vivos. Devido à importância da água para o processo fotossintético, geralmente é encontrada uma relação positiva entre produtividade e precipitação anual, no entanto, a partir de determinado limiar (3000 mm/ano) essa relação se torna negativa (BOISVENUE; RUNNING, 2006; SCHUUR, 2003; TAYLOR et al., 2017). Esse efeito negativo pode ser devido à lixiviação de nutrientes e redução de oxigênio disponível no solo, bem como devido ao bloqueio da radiação devido a elevada nebulosidade (SCHUUR, 2003). A interação entre temperatura média anual e precipitação também é um importante preditor da produtividade primária e da ciclagem de carbono (TAYLOR et al., 2017). Sob menores temperaturas médias anuais (até 20ºC), a precipitação pode ter efeito negativo, principalmente em altitude elevadas, onde o solo pode saturar, levando a anoxia (TAYLOR et al., 2017).

O aumento na concentração de CO_2 na atmosfera teoricamente pode ter um efeito positivo na produtividade primária já que uma quantidade maior de CO_2 estaria disponível para a fotossíntese (HUNTINGFORD et al., 2013; LEWIS et al., 2009). Esse fenômeno é chamado de fertilização da atmosfera e vêm sendo foco de diversos estudos nas últimas décadas. Dentro desse contexto, o efeito positivo da concentração de CO_2 na fotossíntese, seria maior que o efeito do aumento de temperatura (que ocorre devido ao aumento da contração do CO_2) na respiração. As principais questões relacionadas à fertilização da atmosfera são em relação às respostas fisiológicas das plantas e da resiliência dos ecossistemas e florestas aos aumentos nas concentrações de CO_2 (HOFHANSL et al., 2016; LEWIS et al., 2009). Comparando diversos modelos biogeoclimáticos, Huntingford et al. (2013), encontrou que apenas as florestas tropicais da América perderão biomassa até o final do século XXI, enquanto as florestas Asiáticas e Africanas serão resilientes, no entanto, ainda existem muitas incertezas devido às diferentes respostas fisiológicas de diferentes tipos de florestas e espécies (CORLETT, 2016; MCDOWELL et al., 2018). O aumento de CO_2 disponível para as plantas também atuaria no sentido de aumentar a eficiência no uso da água na fotossíntese, no entanto, outras evidências sugerem que o aumento na concentração de CO_2 pode influenciar a produtividade maneira negativa (MCDOWELL et al., 2018). Os aumentos nas taxas de crescimento provocados pela maior quantidade de CO_2 disponível para a fotossíntese podem acelerar a dinâmica sucessional e a proliferação de lianas, aumentando a competição por recursos, e então diminuindo o crescimento e aumentando a mortalidade de árvores (MCDOWELL et al., 2018). Além da competição, pode ocorrer uma aclimatação aos maiores níveis de CO_2, maior exposição a ventos e às implicações fisiológicas de possuir maior tamanho e altura (MCDOWELL et al.,

2018). Além dos efeitos individuais do CO_2, podem ocorrer efeitos interativos entre aumentos na concentração de CO_2 e disponibilidade de nutrientes, como nitrogênio; onde a limitação de nitrogênio suprime a resposta das plantas aos aumentos da concentração de CO_2 (NORBY et al., 2010).

Os nutrientes também desempenham um papel fundamental na produtividade e nos estoques de carbono em florestas (NORBY et al., 2010; TURNER; BRENES-ARGUEDAS; CONDIT, 2018). O fósforo é um nutriente essencial para o metabolismo vegetal, já que constitui o nucleotídeo ATP, responsável pelo armazenamento de energia em suas ligações químicas. Portanto a limitação de fósforo é amplamente debatida, já que algumas espécies desenvolveram estratégias para lidar com a baixa disponibilidade desse nutriente (TURNER; BRENES-ARGUEDAS; CONDIT, 2018). Embora algumas espécies sejam afetadas pela baixa disponibilidade de fósforo, a comunidade como um todo seria resiliente devido às espécies tolerantes à escassez do nutriente (TURNER; BRENES-ARGUEDAS; CONDIT, 2018). Devido à essa adaptação, existe um paradigma relacionado aos efeitos da limitação de fósforo na produtividade vegetal, especialmente devido as interações com a disponibilidade de outros nutrientes, como o nitrogênio (DALLING et al., 2016). Os efeitos da limitação de fósforo também podem variar de acordo com classe etária e grupos funcionais, podendo ser maior em indivíduos mais jovens (ALVAREZ-CLARE; MACK; BROOKS, 2013). No entanto, na meta-análise realizada por Cleveland et al. (2011), fósforo apresentou um efeito positivo e importante na produtividade. Assim como o fósforo, o nitrogênio é um nutriente crucial para o crescimento vegetal, já que constitui a molécula de clorofila, sendo, portanto, um nutriente importante para o funcionamento dos ecossistemas (ELSER et al., 2007). A limitação de nitrogênio, pode limitar a produtividade vegetal devido à importância do nutriente para o metabolismo de seres fotossintetizantes (ELSER et al., 2007), bem como interagir com concentrações de CO_2, limitando o crescimento vegetal (NORBY et al., 2010). Portanto, de maneira geral, a fertilidade do solo tem efeito positivo na produtividade primária e estoques de carbono devido à importância dos nutrientes para o metabolismo das plantas (CLEVELAND et al., 2011).

Dentre os componentes dos estoques e da estocagem de carbono, pode-se destacar a mortalidade de árvores, que pode possuir um papel mais importante que o crescimento na predição de estoques de carbono e produtividade em florestas tropicais (CORLETT, 2016; JOHNSON et al., 2016; MCDOWELL et al., 2018). Os efeitos das mudanças nas condições e na disponibilidade de recursos vêm provocado aumento na mortalidade de árvores, com efeitos negativos na produtividade primária e nos estoques de carbono, especialmente na bacia

Amazônica, onde a mortalidade vem aumentando nas últimas décadas (MCDOWELL et al., 2018). Diversas mudanças ambientais podem agir e interagir para determinar a mortalidade de árvores, como os aumentos de temperatura e no déficit de pressão de vapor que aumentam a mortalidade em escala global devido aos seus efeitos no metabolismo vegetal (ANDEREGG et al., 2016; MCDOWELL et al., 2018). Os aumentos na duração dos períodos de seca também possuem efeitos positivos na mortalidade de árvores, principalmente devido a falha hidráulica e efeitos nas taxas de respiração, onde as árvores de maior porte são mais afetadas, acarretando perdas significativas de carbono (CORLETT, 2016; MCDOWELL et al., 2018). Embora os aumentos das concentrações de CO_2 possam acelerar o crescimento, eles aumentam a mortalidade de maneira indireta, já que os aumentos nas taxas de crescimento aceleram a dinâmica sucessional, aumentando a competição por recursos (MCDOWELL et al., 2018). O acréscimo nas taxas de crescimento provocados pelo aumento nas concentrações de CO_2 também podem causar mortalidade devido a maior velocidade com que as árvores podem atingir maiores alturas, deixando-as sujeitas as adversidades relacionadas a copa, como maior incidência de vento, e aos impactos fisiológicos relacionados a árvores de grande porte (MCDOWELL et al., 2018). Além desses fatores, a competição com lianas (que aumentam a sua abundância devido à seca e aumentos nas concentrações de CO_2), fogo e vento, constituem importantes preditores da mortalidade de árvores (MCDOWELL et al., 2018). Os fatores que determinam a mortalidade possuem efeitos semelhantes no crescimento vegetal, no sentido de que algumas árvores podem sobreviver nessas novas condições, mas teriam seu crescimento reduzido devido a competição e escassez de recursos. No entanto, todos os fatores interagem para determinar os padrões observados, sendo complexo avaliar a importância de cada um e predizer a mortalidade em um mundo em transformação. Em síntese, é provável que as mudanças climáticas afetem negativamente os estoques de carbono e a produtividade das florestais tropicais, principalmente devido às respostas fisiológicas dos indivíduos, populações e comunidades (ANDEREGG et al., 2016; FENG et al., 2018). No entanto, para compreender melhor esses processos e realizar predições confiáveis para cenários futuros, necessita-se que dados robustos sejam coletados em campo, a fim de prover informações mais detalhadas para a tomada de decisão em âmbito público.

3 CONSIDERAÇÕES FINAIS

É extremamente necessário preencher a lacuna de conhecimento em relação à dinâmica do carbono em florestas não-amazônicas, que se encontram grande parte fragmentadas e ameaçadas pela expansão agropecuária. Esse conhecimento é essencial para dimensionar e predizer o tamanho dos estoques e do sumidouro de carbono dessas florestas, para assim subsidiar políticas de conservação e tomadas de decisão no âmbito público/político. Ademais, são raros os estudos que contam com longos períodos de monitoramento em grandes escalas espaciais dessas florestas. A partir dos dados espaço-temporais de florestas tropicais extra-amazônicas é possível observar as respostas dessas florestas ao longo das últimas décadas, e então entender e predizer os estoques e o sumidouro de carbono. Essas informações seriam de grande relevância para a comunidade científica e política, no sentido de proteger e preservar o papel importante que essas florestas desempenham a partir da provisão de serviços ecossistêmicos, essenciais à manutenção de aspectos ambientais, sociais e econômicos, não só das regiões onde estão inseridas, mas de todo o planeta.

REFERÊNCIAS

ALLEN, K. et al. Will seasonally dry tropical forests be sensitive or resistant to future changes in rainfall regimes? **Environmental Research Letters**, v. 12, n. 2, p. 023001, 2017.

ÁLVAREZ-DÁVILA, E. et al. Forest biomass density across large climate gradients in northern South America is related to water availability but not with temperature. **PloS One**, v. 12, n. 3, p. e0171072, 2017.

ALVAREZ-CLARE, S.; MACK, M. C.; BROOKS, M. A direct test of nitrogen and phosphorus limitation to net primary productivity in a lowland tropical wet forest. **Ecology**, v. 94, n. 7, p. 1540-1551, 2013.

ANDEREGG, W. R. L. et al. When a tree dies in the forest: scaling climate-driven tree mortality to ecosystem water and carbon fluxes. **Ecosystems**, v. 19, n. 6, p. 1133-1147, 2016.

ARCHER, D. **The Global Carbon Cycle.** New Jersey: Princeton University Press, 2010.

ARRUDA, D. M. et al. Combining climatic and soil properties better predicts covers of Brazilian biomes. **The Science of Nature**, v. 104, n. 3-4, p. 32-42, 2017a.

ARRUDA, D. M. et al. Vegetation cover of Brazil in the last 21 ka: New insights into the Amazonian refugia and Pleistocenic arc hypotheses. **Global Ecology and Biogeography**, v. 27, n. 1, p. 47-56, 2017b.

BACCINI, A. et al. Tropical forests are a net carbon source based on aboveground measurements of gain and loss. **Science**, v. 358, n. 6360, p. 230-234, 2017.

BOISVENUE, C.; RUNNING, S. W. Impacts of climate change on natural forest productivity–evidence since the middle of the 20th century. **Global Change Biology**, v. 12, n. 5, p. 862-882, 2006.

BUENO, M. L. et al. The environmental triangle of the Cerrado Domain: Ecological factors driving shifts in tree species composition between forests and savannas. **Journal of Ecology**, v. 106, n. 5, p. 2109-2120, 2018.

CARVALHO, C. J. B.; ALMEIDA E. A. B. (Org.). **Biogeografia da América do Sul:** padrões & processos. São Paulo: Roca, 2011.

CHASE, M. W. et al. An update of the Angiosperm Phylogeny Group classification for the orders and families of flowering plants: APG IV. **Botanical Journal of the Linnean Society**, v. 181, n. 1, p. 1-20, 2016.

CHAVE, J. et al. Tree allometry and improved estimation of carbon stocks and balance in tropical forests. **Oecologia**, v. 145, n. 1, p. 87-99, 2005.

CHAVE, J. et al. Towards a worldwide wood economics spectrum. **Ecology Letters**, v. 12, n. 4, p. 351-366, 2009.

CHAVE, J. et al. Improved allometric models to estimate the aboveground biomass of tropical trees. **Global Change Biology**, v. 20, n. 10, p. 3177-3190, 2014.

CLEVELAND, C. C. et al. Relationships among net primary productivity, nutrients and climate in tropical rain forest: a pan-tropical analysis. **Ecology Letters**, v. 14, n. 9, p. 939-947, 2011.

COLINVAUX, P. A.; OLIVEIRA, P. E.; BUSH, M. B. Amazonian and neotropical plant communities on glacial time-scales: the failure of the aridity and refuge hypotheses. **Quaternary Science Reviews**, v. 19, n. 1-5, p. 141-169, 2000.

COLLEVATTI, R. G. et al. Drawbacks to palaeodistribution modelling: the case of South American seasonally dry forests. **Journal of Biogeography**, v. 40, n. 2, p. 345-358, 2013.

COLOMBO, A. F.; JOLY, C. A. Brazilian Atlantic Forest *lato sensu*: the most ancient Brazilian forest, and a biodiversity hotspot, is highly threatened by climate change. **Brazilian Journal of Biology**, v. 70, n. 3, p. 697-708, 2010.

CORLETT, R. T. The impacts of droughts in tropical forests. **Trends in Plant Science**, v. 21, n. 7, p. 584-593, 2016.

COSTA, G. C. et al. Biome stability in South America over the last 30 kyr: Inferences from long-term vegetation dynamics and habitat modelling. **Global ecology and biogeography**, v. 27, n. 3, p. 285-297, 2017.

DALLING, J. W. et al. Nutrient availability in tropical rain forests: the paradigm of phosphorus limitation. In: GOLDSTEIN G.; SANTIAGO L. (Ed.). **Tropical Tree Physiology**. 6v., Cham: Springer, p. 261-273, 2016.

DLUGOKENCKY, E.; TANS, P. **Trends in atmospheric carbon dioxide, National Oceanic & Atmospheric Administration, Earth System Research Laboratory (NOAA/ESRL).** Disponível em: <http://www.esrl.noaa.gov/gmd/ccgg/trends/global.html> Acesso em: março, 2019.

ELSER, J. J. et al. Global analysis of nitrogen and phosphorus limitation of primary producers in freshwater, marine and terrestrial ecosystems. **Ecology Letters**, v. 10, n. 12, p. 1135-1142, 2007.

FENG, X. et al. Improving predictions of tropical forest response to climate change through integration of field studies and ecosystem modeling. **Global Change Biology**, v. 24, n. 1, p. e213-e232, 2018.

GAZOL, A. et al. Forest resilience to drought varies across biomes. **Global Change Biology**, v. 24, n. 5, p. 2143-2158, 2018.

HAFFER, J. Speciation in Amazonian forest birds. **Science**, v. 165, n. 3889, p. 131-137, 1969.

HALLIDAY, A. N. The origin and earliest history of the Earth. In: DAVIS, A. M. (Ed.). **Planets, Asteriods, Comets and The Solar System.** Elsevier, 2014. p. 149-211.

HENGL, T. et al. SoilGrids1km - global soil information based on automated mapping. **PloS One**, v. 9, n. 8, p. e105992, 2014.

HIJMANS, R. J. et al. Very high resolution interpolated climate surfaces for global land areas. **International Journal of Climatology:** A Journal of the Royal Meteorological Society, v. 25, n. 15, p. 1965-1978, 2005.

HOFHANSL, F. et al. Amazon forest ecosystem responses to elevated atmospheric CO_2 and alterations in nutrient availability: filling the gaps with model-experiment integration. **Frontiers in Earth Science**, v. 4, n. 19, p. 1-9, 2016.

HOPKINS, W. G.; HÜNER, N. P. A. **Introducction to Plant Physiology**. 3rd ed., Hoboken: John Wiley & Sons, 2004.

Hubau, W., Lewis, S.L., Phillips, O.L. *et al.* Asynchronous carbon sink saturation in African and Amazonian tropical forests. *Nature* **579,** 80–87,2020. https://doi.org/10.1038/s41586-020-2035-0

HUNTINGFORD, C. et al. Simulated resilience of tropical rainforests to CO 2-induced climate change. **Nature Geoscience**, v. 6, n. 4, p. 268-273, 2013.

JOHNSON, M. O. et al. Variation in stem mortality rates determines patterns of above-ground biomass in Amazonian forests: implications for dynamic global vegetation models. **Global Change Biology**, v. 22, n. 12, p. 3996-4013, 2016.

KEENAN, R. J. et al. Dynamics of global forest area: Results from the FAO Global Forest Resources Assessment 2015. **Forest Ecology and Management**, v. 352, n. 1, p. 9-20, 2015.

KEENAN, T. F.; WILLIAMS, C. A. The terrestrial carbon sink. **Annual Review of Environment and Resources**, v. 43, n. 1, p. 219-243, 2018.

KNAPP, A. K.; SMITH, M. D. Variation among biomes in temporal dynamics of aboveground primary production. **Science**, v. 291, n. 5503, p. 481-484, 2001.

LE QUÉRÉ, C. et al. Global carbon budget 2018. **Earth System Science Data**, v. 10, n. 4, p. 2141-2194, 2018.

LEITE, Y. L. R. et al. Neotropical forest expansion during the last glacial period challenges refuge hypothesis. **Proceedings of the National Academy of Sciences**, v. 113, n. 4, p. 1008-1013, 2016.

LEWIS, S. L. Tropical forests and the changing earth system. **Philosophical Transactions of the Royal Society B**: Biological Sciences, v. 361, n. 1465, p. 195-210, 2006.

LEWIS, S. L. et al. Changing ecology of tropical forests: evidence and drivers. **Annual Review of Ecology, Evolution, and Systematics**, v. 40, n. 1, p. 529-549, 2009.

LI, W. et al. Recent changes in global photosynthesis and terrestrial ecosystem respiration constrained from multiple observations. **Geophysical Research Letters**, v. 45, n. 2, p. 1058-1068, 2018.

LYRA, A. A.; CHOU, S. C.; SAMPAIO, G. O. Sensitivity of the Amazon biome to high resolution climate change projections. **Acta Amazonica**, v. 46, n. 2, p. 175-188, 2016.

MAGRIN, G. O. et al. Central and South America. In: BARROS, V. R. et al. (Ed.). **Climate Change 2014:** Impacts, adaptation, and vulnerability - Regional aspects. Cambridge: Cambridge University Press., p. 1499-1566, 2014.

MALHI, Y. The productivity, metabolism and carbon cycle of tropical forest vegetation. **Journal of Ecology**, v. 100, n. 1, p. 65-75, 2012.

MCDOWELL, N. et al. Drivers and mechanisms of tree mortality in moist tropical forests. **New Phytologist**, v. 219, n. 3, p. 851-869, 2018.

MCELWAIN, J. C. Paleobotany and global change: important lessons for species to biomes from vegetation responses to past global change. **Annual Review of Plant Biology**, v. 69, n. 1, p. 761-787, 2018.

MEIR, P.; WOODWARD, F. I. Amazonian rain forests and drought: response and vulnerability. **New Phytologist**, v. 187, n. 3, p. 553-557, 2010.

MITCHARD, E. T. A. The tropical forest carbon cycle and climate change. **Nature**, v. 559, n. 7715, p. 527, 2018.

MONCRIEFF, G. R.; BOND, W. J.; HIGGINS, S. I. Revising the biome concept for understanding and predicting global change impacts. **Journal of Biogeography**, v. 43, n. 5, p. 863-873, 2016.

NEVES, D. M. et al. Dissecting a biodiversity hotspot: The importance of environmentally marginal habitats in the Atlantic Forest Domain of South America. **Diversity and Distributions**, v. 23, n. 8, p. 898-909, 2017.

NORBY, R. J. et al. CO_2 enhancement of forest productivity constrained by limited nitrogen availability. **Proceedings of the National Academy of Sciences**, v. 107, n. 45, p. 19368-19373, 2010.

PACHAURI R. K.; MEYER L. A. (eds.) **Climate change 2014:** the physical science basis: Working Group I contribution to the Fifth assessment report of the Intergovernmental Panel on Climate Change. Geneva: IPCC, 2014.

PAN, Y. et al. A large and persistent carbon sink in the world's forests. **Science**, v. 333, n. 6045, p. 988-993, 2011.

PAN, Y. et al. The structure, distribution, and biomass of the world's forests. **Annual Review of Ecology, Evolution, and Systematics**, v. 44, n. 1, p. 593-622, 2013.

PAUSAS, J. G.; RIBEIRO, E. Fire and plant diversity at the global scale. **Global Ecology and Biogeography**, v. 26, n. 8, p. 889-897, 2017.

PENNINGTON, R. T.; PRADO, D. E.; PENDRY, C. A. Neotropical seasonally dry forests and Quaternary vegetation changes. **Journal of Biogeography**, v. 27, n. 2, p. 261-273, 2000.

PENNINGTON, R. T.; LAVIN, M.; OLIVEIRA-FILHO, A. Woody plant diversity, evolution, and ecology in the tropics: perspectives from seasonally dry tropical forests. **Annual Review of Ecology, Evolution, and Systematics**, v. 40, n. 1, p. 437-457, 2009.

PRADO, D. E.; GIBBS, P. E. Patterns of species distributions in the dry seasonal forests of South America. **Annals of the Missouri Botanical Garden**, v. 80, n. 4, p. 902-927, 1993.

RANGEL, T. F. et al. Modeling the ecology and evolution of biodiversity: biogeographical cradles, museums, and graves. **Science**, v. 361, n. 6399, p. eaar5452, 2018.

ROBERTS, P.; BOIVIN, N.; KAPLAN, J. O. Finding the anthropocene in tropical forests. **Anthropocene**, v. 23, n. 1, p. 5-16, 2018.

SCARANO, F. R.; CEOTTO, P. Brazilian Atlantic forest: impact, vulnerability, and adaptation to climate change. **Biodiversity and Conservation**, v. 24, n. 9, p. 2319-2331, 2015.

SCHUUR, E. A. G. Productivity and global climate revisited: the sensitivity of tropical forest growth to precipitation. **Ecology**, v. 84, n. 5, p. 1165-1170, 2003.

SCOLFORO, H. F. et al. Spatial interpolators for improving the mapping of carbon stock of the arboreal vegetation in Brazilian biomes of Atlantic forest and Savanna. **Forest Ecology and Management**, v. 376, n.1, p. 24-35, 2016.

SCOTESE, C. R. Late Proterozoic plate tectonics and palaeogeography: a tale of two supercontinents, Rodinia and Pannotia. **Geological Society, London, Special Publications**, v. 326, n. 1, p. 67-83, 2009.

SHEIL, D.; MAY, R. M. Mortality and recruitment rate evaluations in heterogeneous tropical forests. **Journal of Ecology**, v. 84, n. 1, p. 91-100, 1996.

SULLIVAN, M. J. P. et al. Diversity and carbon storage across the tropical forest biome. **Scientific Reports**, v. 7, n. 39102, p. 1-12, 2017.

SULLIVAN, M. J. P. et al. Long-term thermal sensitivity of Earth's tropical forests. *Science* **368**, 869–874, 2020.

TALBOT, J. et al. Methods to estimate aboveground wood productivity from long-term forest inventory plots. **Forest Ecology and Management**, v. 320, n. 1, p. 30-38, 2014.

TAYLOR, P. G. et al. Temperature and rainfall interact to control carbon cycling in tropical forests. **Ecology Letters**, v. 20, n. 6, p. 779-788, 2017.

TERRA, M. C. N. S. et al. Tree dominance and diversity in Minas Gerais, Brazil. **Biodiversity and Conservation**, v. 26, n. 9, p. 2133-2153, 2017.

TURNER, B. L.; BRENES-ARGUEDAS, T.; CONDIT, R. Pervasive phosphorus limitation of tree species but not communities in tropical forests. **Nature**, v. 555, n. 7696, p. 367-370, 2018.

WERNECK, F. P. et al. Revisiting the historical distribution of Seasonally Dry Tropical Forests: new insights based on palaeodistribution modelling and palynological evidencegeb. **Global Ecology and Biogeography**, v. 20, n. 2, p. 272-288, 2011.

WHITNEY, B. S. et al. A 45 kyr palaeoclimate record from the lowland interior of tropical South America. **Palaeogeography, Palaeoclimatology, Palaeoecology**, v. 307, n. 1-4, p. 177-192, 2011.

ZANNE, A. E. et al. **Global wood density database**. Dryad Digital Repository, 2009. Disponível em: <http://datadryad.org/handle/10255/dryad.235>. Acesso em: julho, 2019.

ZUMDAHL, S. S.; ZUMDAHL, S. A.; DECOSTE, D. J. **Chemistry**. 10th ed., Cengage Learning, 2017.

ZWIENER, V. P. et al. Climate change as a driver of biotic homogenization of woody plants in the Atlantic Forest. **Global Ecology and Biogeography**, v. 27, n. 3, p. 298-309, 2017.

SEGUNDA PARTE – Artigo

(publicado no periódico *Science Advances*)

The carbon sink of tropical seasonal forests in southeastern Brazil can be under threat

Vinicius Andrade Maia[1]*, Alisson Borges Miranda Santos[1], Natalia de Aguiar-Campos[1], Cleber Rodrigo de Souza[1], Matheus Coutinho Freitas de Oliveira[1], Polyanne Aparecida Coelho[1], Jean Daniel Morel[1], Lauana Silva da Costa[1], Camila Lais Farrapo[1], Nathalle Cristine Alencar Fagundes[1],[2],[3], Gabriela Gomes Pires de Paula[1], Paola Ferreira Santos[2], Fernanda Moreira Gianasi[2], Wilder Bento da Silva[1], Fernanda de Oliveira[2], Diego Teixeira Girardelli[1], Felipe de Carvalho Araujo[1], [2], Taynara Andrade Vilela[1], Rafaella Tavares Pereira[1], Lidiany Carolina Arantes da Silva[1], Gisele Cristina de Oliveira Menino[4], Paulo Oswaldo Garcia[5], Marco Aurelio Leite Fontes[1], Rubens Manoel dos Santos[1],[2]*

[1]Departamento de Ciencias Florestais, Universidade Federal de Lavras, P.O. Box 3037, Lavras, MG 37200-900, Brazil.
[2]Departamento de Ciencias Biologicas, Universidade Federal de Lavras, P.O. Box 3037, Lavras, MG 37200-900, Brazil.
[3]Universidade do Estado de Minas Gerais, P.O. Box 431, Ituiutaba, MG 38302-192, Brazil.
[4]Instituto Federal Goiano, P.O. Box 66, Rio Verde, GO 75901-970, Brazil.
[5]Instituto Federal de Educacao, Ciencia e Tecnologia Sul de Minas Gerais–Campus Muzambinho, P.O. Box 02, Muzambinho, MG 37890-000, Brazil.

*Corresponding author. Email: vinicius.a.maia77@gmail.com (V.A.M.); rubensmanoel@ufla.br (R.M.d.S.)

Tropical forests have played an important role as a carbon sink over time. However, the carbon dynamics of Brazilian non-Amazon tropical forests are still not well understood. Here, we used data from 32 tropical seasonal forest sites, monitored from 1987 to 2020 (mean site monitoring length, ~15 years) to investigate their long-term trends in carbon stocks and sinks. Our results highlight a long-term decline in the net carbon sink (0.13 Mg C ha−1 year−1) caused by decreasing carbon gains (2.6% by year) and increasing carbon losses (3.4% by year). The driest and warmest sites are experiencing the most severe carbon sink decline and have already moved from carbon sinks to carbon sources. Because of the importance of the terrestrial carbon sink for the global climate, policies are needed to mitigate the emission of greenhouse gases and to restore and protect tropical seasonal forests.

INTRODUCTION

Tropical forests have a key role in the global carbon dynamics by accounting for one-third of the terrestrial gross primary production and one-half of the terrestrial stored carbon (*1*, *2*). Increasing atmospheric CO2 concentration, rising temperatures, drought events, and deforestation are expected to affect ecosystem functioning through plant physiological responses and forest loss over the coming decades (*3*–*7*). How tropical forests will respond to increasing atmospheric CO2 concentration and climate change are sources of uncertainty in predicting their future carbon stocks and net primary productivity (*6*, *8*). Among tropical forests, the ones under stressful conditions, such as the seasonally dry tropical forests (SDTFs) that endure periodic droughts, can be vulnerable to these environmental changes because they are already at the edge of climate niches to sustain forest formations with high biomass (*9*, *10*). Brazil has been the largest source of carbon emissions from gross deforestation up to 2013: In 2013 alone, 192,000 ha of Caatinga forests (where the largest continuous extent of neotropical SDTFs is located) and 24,000 ha of Atlantic forests were deforested (*11*). An aggravating factor is that only 6.2% of Brazilian SDTF extent is protected (*12*). In this context, it is crucial to advance our understanding of the carbon sink of these forests (*9*, *10*).

Over recent decades, the terrestrial carbon sink has been increasing globally (*13*, *14*). This phenomenon is possibly explained by the increases in atmospheric CO2 concentration (CO2 fertilization), which is expected to enhance plant growth (*6*, *13*). Carbon dioxide has a key role in photosynthesis and can potentially increase water use efficiency (WUE) by reducing stomata conductance (*15*, *16*). In this context, the increases in atmospheric CO2 concentration are thought to have enhanced photosynthesis more than rising temperatures have enhanced respiration (*17*, *18*). Hence, drought-related stress on plant growth would be understated by rising atmospheric CO2 concentration. However, the mechanisms involved in the feedbacks among vegetation, atmospheric CO2, and climate are complex. For example, the increase in photosynthesis and WUE led by rising atmospheric CO2 concentration does not necessarily promote stand growth because of the effects of other co-occurring factors (*19*). The effects of increasing drought, rising temperatures, competition, and physiological acclimation to higher levels of CO2 can constrain tree growth and also lead to tree mortality (*3*, *5*, *20*, *21*). Therefore, it is difficult to disentangle the effects of climate fluctuations and rising CO2 on carbon dynamics because these factors covary and can interact over time (*5*).

While recent studies have shown a long-term decline in the Amazon rainforest carbon sink, mostly driven by climate-induced tree mortality (*6*, *22*), others have predicted that tropical rainforest carbon sink may be resilient to climate change in the next decades (*18*). However, it remains uncertain how Brazilian seasonal forests (which are already exposed to drought), such as deciduous forests (SDTFs) and semideciduous forests, have responded to the increasing levels of atmospheric CO2 and climate fluctuations over time (*4*, *9*, *23*). To assess how these forests are behaving over time, we use long-term seasonal forest census data from southeastern Brazil (Figs. 1 and 2) to investigate the long-term trends of carbon stocks, gains, losses, and net carbon sink. We draw our inferences from 95 census intervals nested within 32 sites, ranging between 1987 and 2020 (mean site total monitoring length, ~15 years). The spatial (number of sites and sampled area) and temporal (interval length and total monitoring time) sampling efforts varied among sites and forest types; this variability is depicted in Fig. 2, figs. S1 and S2, and Materials and Methods. The forest sites used here are in advanced successional stages, free from fire, flood, landslides, and human disturbances at least for

decades before the first census of each site. The data encompass a wide environmental space and three forest types (deciduous, evergreen, and semideciduous forests) (Fig. 2 and figs. S3 and S4), allowing us to investigate whether forests under different climates have differed in their long-term trends. In addition to the rising atmospheric CO2 concentration [parts per million (ppm)] and CO2 change (ppm year−1) over time, mean annual temperature (MAT) and mean annual precipitation (MAP) have shown an unstable temporal trend in our data (Fig. 3). Therefore, we used time (year) as a proxy of the effects of rising CO2, climate fluctuations, and other unmeasured confounding effects over time. We did this because these factors can be codependent and correlated over time, being difficult to disentangle their individual effects. We fitted statistical models to assess the general long-term trends of carbon dynamics, as well as the long-term trends by forest type, and to test whether climate mediates these long-term trends. More specifically, we tested whether sites under different climate conditions have differed in their long-term trends. In this sense, we expected the long-term trends of sites under drier and warmer conditions to differ from the long-term trends of sites under wetter and colder conditions.

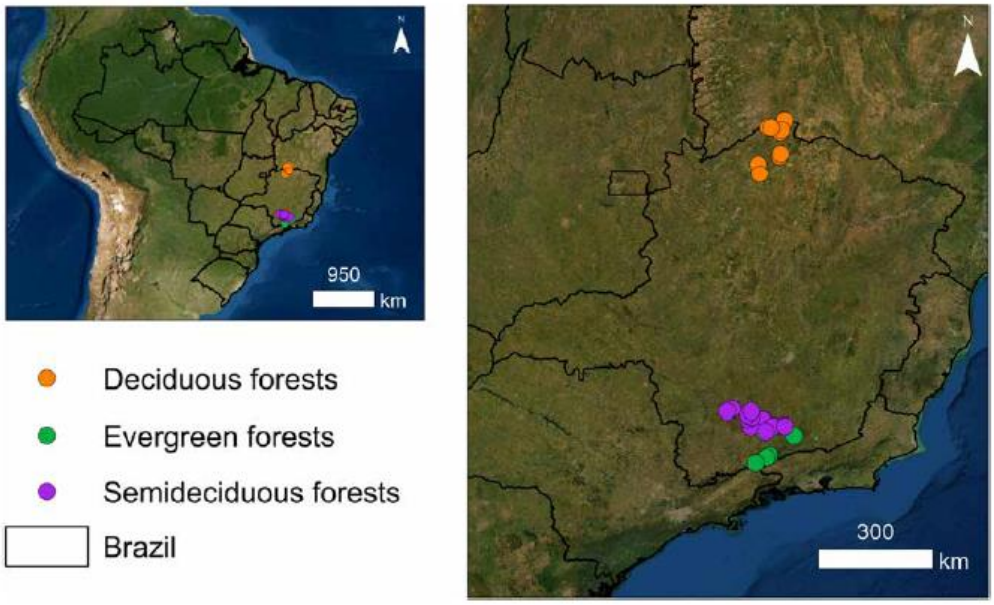

Fig. 1. Spatial location of the sampled sites in South America. The 32 sampled sites belong to three forest types: deciduous forests (*n* = 11), evergreen forests (*n* = 5), and semideciduous forests (*n* = 16) (Sentinel-2 image).

RESULTS

Both MAT and MAP fluctuated over time (Fig. 3, A and B). MAT showed a positive trend (0.04°C by year) (Fig. 3A), while MAP showed a negative trend (−10.2 mm by year) (Fig. 3B). Moreover, CO2 change increased almost linearly with time (Fig. 3C). In general, the carbon stocks increased over time until 2013 (~0.67% by year) and then started to decline (Fig. 4A). During most of the time, the net carbon sink was above zero (positive balance between carbon gains and losses), with a slight negative trend; however, in 2013, the net carbon sink became negative (carbon losses exceeded carbon gains) (Fig. 4B), which explains the carbon stock decline after 2013. In general, the net carbon sink decreased by 0.13 Mg C ha^{-1} $year^{-1}$. Carbon gains decreased (~2.6% by year) and carbon losses increased (~3.4% by

year) almost linearly over time (Fig. 4, C and D). Predictions for the years 2013 and 2018 together with the observed mean, maximum, and minimum values of each carbon dynamics variable can be found in Table 1.

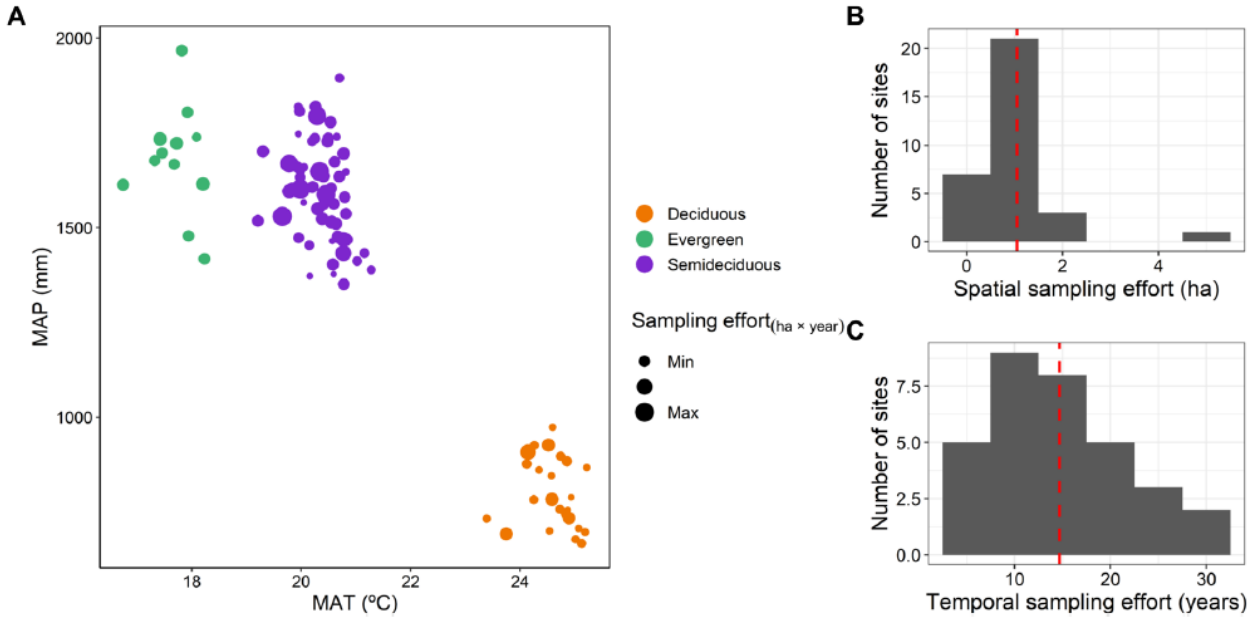

Fig. 2. Distribution of sites and forest types over the climate space and spatial-temporal sampling efforts. (**A**) Distribution of the sites and forest types within the climate space represented by mean annual temperature (MAT) and mean annual precipitation (MAP). The points are census intervals (n = 95), and their sizes are proportional to the site sampled area (mean, 1.05 ha) times interval length (mean, 5 years). (**B**) Frequency of site sampled areas (n = 32). The red dashed line is the mean of the sampled area among sites (1.05 ha). (**C**) Frequency of site total monitoring length (n = 32) (year of the last census minus year of first census). The red dashed line is the mean of the total monitoring length among sites (14.7 years).

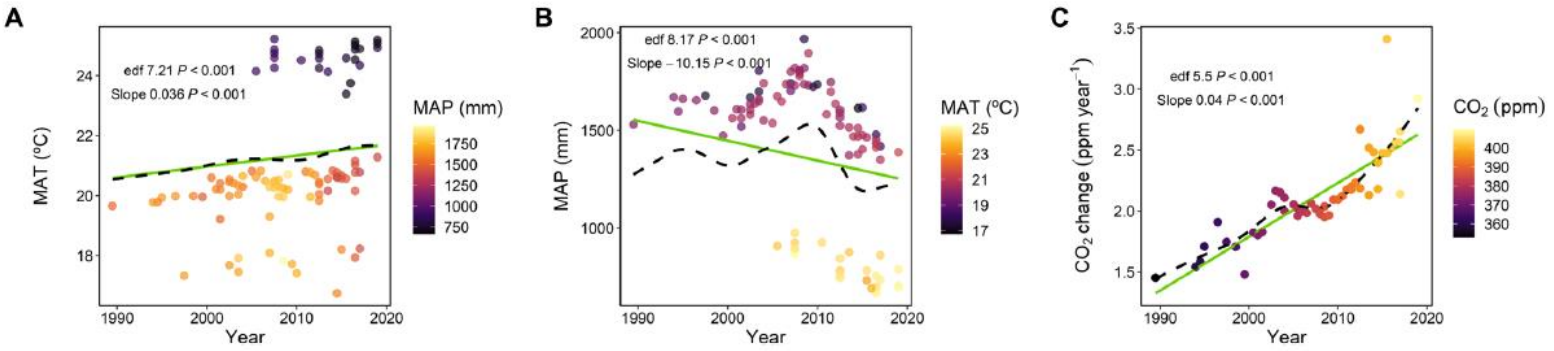

Fig. 3. Long-term trends of the environmental variables. (**A**) MAT, (**B**) MAP, and (**C**) CO2 change. The points are census intervals (n = 95). The black dashed curves were fitted with generalized additive models (GAM, including a random effect of site), and the green solid curves were fitted with LMM (including a random effect of site). Note that if the effective degree of freedom (edf) from GAM is equal to 1, then the relationship is linear.

The long-term trends by forest type revealed that the carbon stocks of the semideciduous forests increased over time, while the carbon stocks of the deciduous and evergreen forests showed a stable trend, whereby the deciduous forests showed a slight (but nonsignificant) decrease (Fig. 5A). All forest types showed a decline in their net carbon sinks over time, with a stronger decline in deciduous forests (Fig. 5B). Carbon gains decreased and carbon losses increased in all forest types, but these trends were more pronounced in the deciduous forests than in other forest types (Fig. 5, C and D).

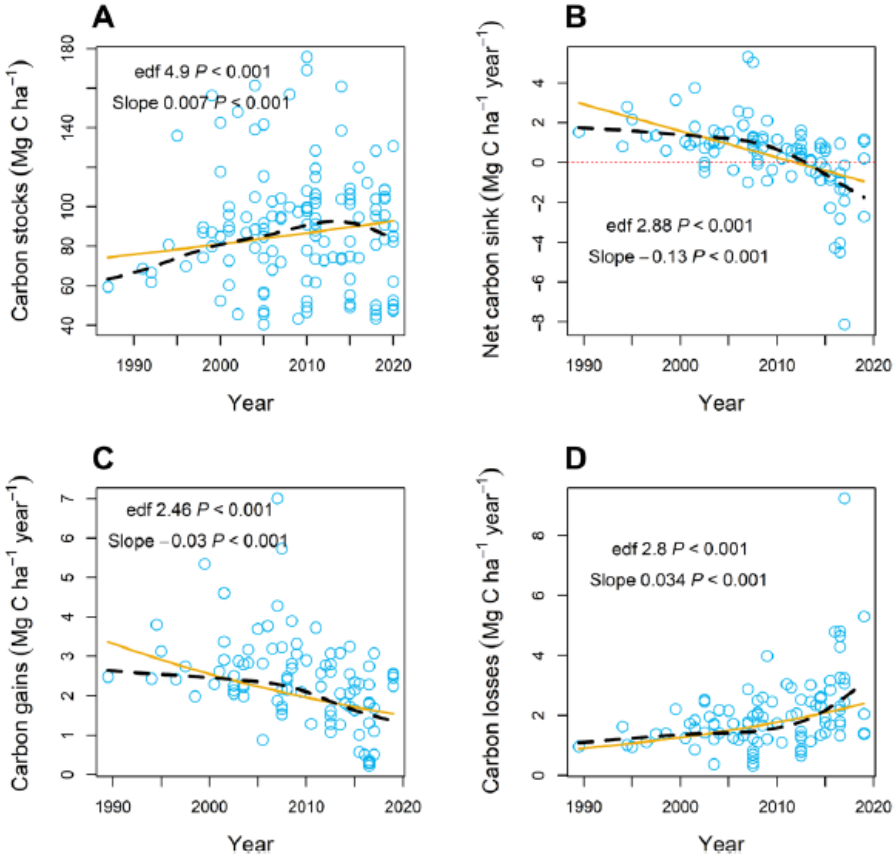

Fig. 4. Long-term trends of carbon stocks and dynamics. (**A**) Carbon stocks, (**B**) net carbon sink, (**C**) carbon gains, and (**D**) carbon losses. In (A), censuses (n = 127) nested within sites (n = 32); in (B) to (D), census intervals (n = 95) nested within sites (n = 32). The black dashed curves were fitted with GAMs (including a random effect of site), and the orange solid curves were fitted with LMMs (including a random effect of site). Note that the slopes of the carbon stock, carbon gain, and carbon loss models were estimated in the logarithmic scale; if the edf (from GAM) is equal to 1, then the relationship is linear.

Table 1. This table shows the observed and predicted (2003 and 2018) means, minimums, and maximums of each carbon dynamics variable. Predictions were obtained from the GAMs (including a random effect of site) (Fig. 4). Data with census intervals (n = 95) nested within sites (n = 32). Note that the minimum and maximum of the predicted net carbon sink are converged toward the mean because the estimated variance between sites was near zero.

Average	Carbon dynamics	Minimum	Mean	Maximum
Observed (1987-2020)	Carbon stocks (Mg C ha^{-1})	40.5	89.3	175.7
	Net carbon sink (Mg C ha^{-1} yr^{-1})	-8.1	0.4	5.3
	Carbon gains (Mg C ha^{-1} yr^{-1})	0.2	2.4	7.0
	Carbon losses (Mg C ha^{-1} yr^{-1})	0.3	2.0	9.2
Predicted (2003)	Carbon stocks (Mg C ha^{-1})	43.5	86.4	160.9
	Net carbon sink (Mg C ha^{-1} yr^{-1})	1.3	1.3	1.3
	Carbon gains (Mg C ha^{-1} yr^{-1})	1.3	2.6	4.2
	Carbon losses (Mg C ha^{-1} yr^{-1})	0.9	1.4	1.7
Predicted (2018)	Carbon stocks (Mg C ha^{-1})	45.7	90.8	169.1
	Net carbon sink (Mg C ha^{-1} yr^{-1})	-1.5	-1.5	-1.5
	Carbon gains (Mg C ha^{-1} yr^{-1})	0.8	1.5	2.5
	Carbon losses (Mg C ha^{-1} yr^{-1})	1.9	2.9	3.5

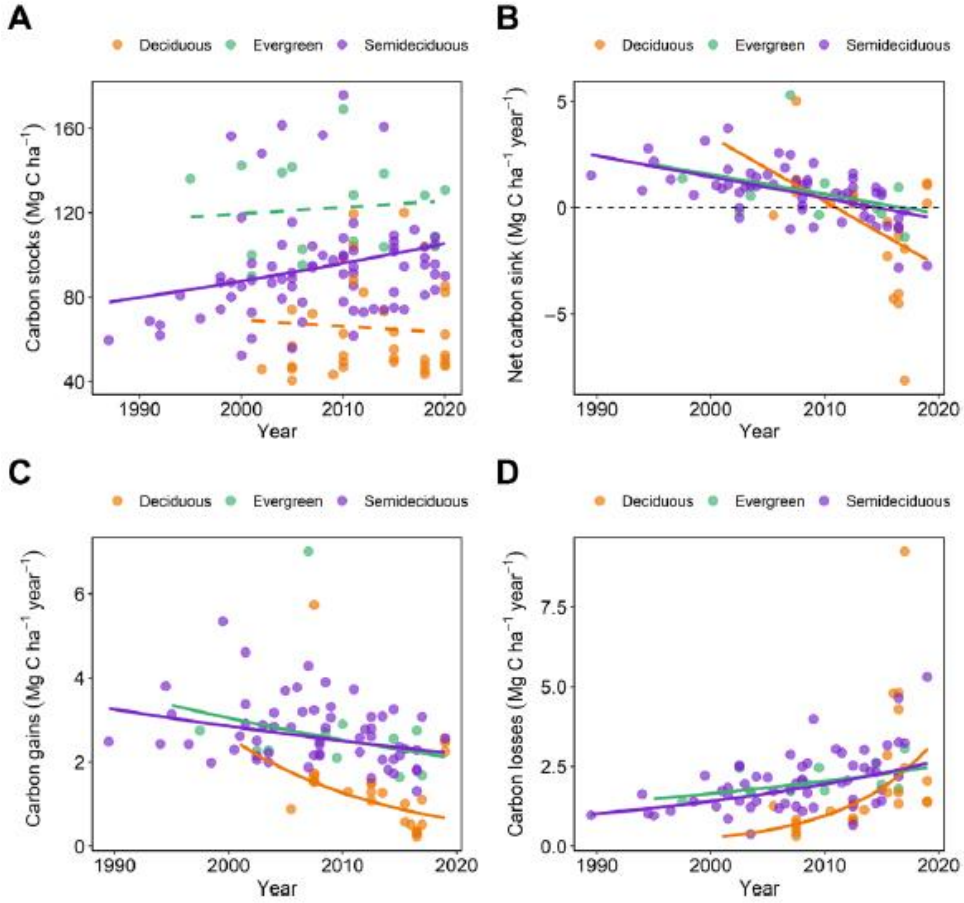

Fig. 5. Long-term trends of carbon stocks and dynamics by forest type. (**A**) Carbon stocks, (**B**) net carbon sink, (**C**) carbon gains, and (**D**) carbon losses. In (A), censuses (n = 127) nested within sites (n = 32); in (B) to (D), census intervals (n = 95) nested within sites (n = 32). The curves were fitted with LMMs (including a random effect of site). Dashed curves are nonsignificant effects (significance level of 0.05).

In the final model, including climate, soil, and time, the forests under different climate conditions differed in their long-term trends (Figs. 6 to 8). Carbon stocks increased over time, except for the driest and warmest sites, in a way that the positive temporal trend of carbon stocks became weaker with decreasing MAP and increasing MAT (Figs. 6A and 7, A and B). Net carbon sink decreased over time, in a way that its negative temporal trend became weaker as MAP increases and MAT decreases (Figs. 6B and 7, C and D). Carbon gains decreased with time, whereby its negative trend became weaker with decreasing MAT and increasing MAP, and became positive under wet conditions (Figs. 6C and 8, A and B). At the same time, carbon losses increased over the years; the temporal trend of carbon losses became weaker with increasing MAP and decreasing MAT (Figs. 6D and 8, C and D).

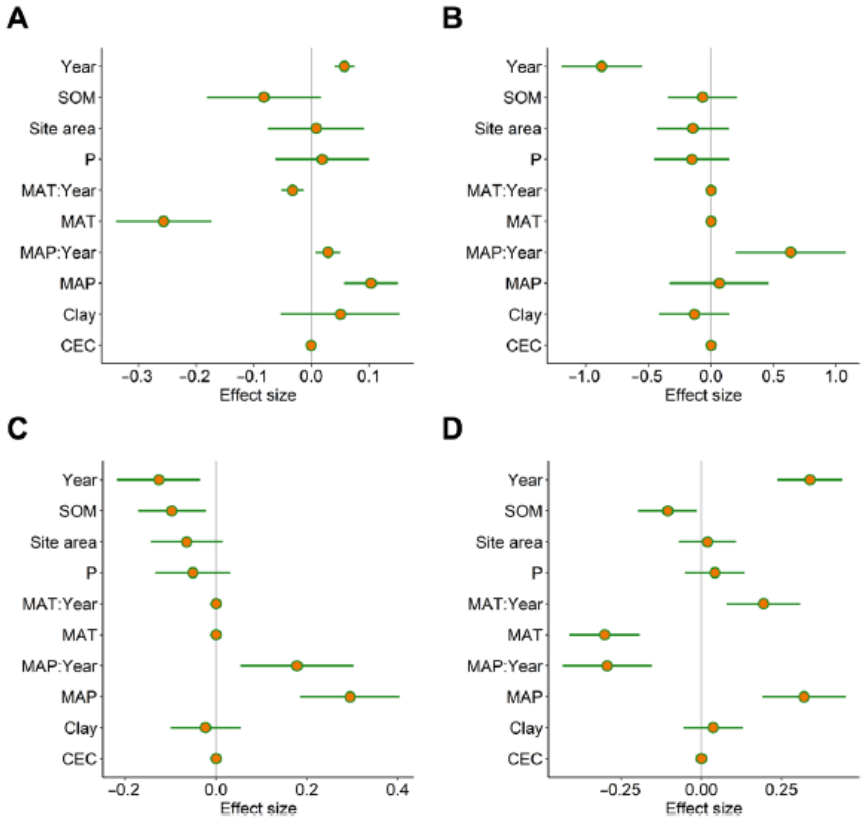

Fig. 6. Averaged models (selected models ΔAICc ≤ 4) containing the effects of time, climate, and soil on carbon stocks and dynamics. (**A**) Carbon stocks (averaged marginal $R2$ = 32.5%), (**B**) net carbon sink (averaged marginal $R2$ = 29.3%), (**C**) carbon gains (averaged marginal $R2$ = 48.6%), and (**D**) carbon losses (averaged marginal $R2$ = 28.7%). Dots are the conditional averaged coefficients with their 95% confidence intervals; the coefficients and confidence intervals of variables not included in the averaged model were set to zero. In (A), censuses (n = 127) nested within sites (n = 32); in (B) to (D), census intervals (n = 95) nested within sites (n = 32). The coefficients were estimated using LMMs (including a random effect of site). The coefficients of the carbon stock, carbon gain, and carbon loss models were estimated in the logarithmic scale, and all models were fitted with scaled predictors.

The effects of climate have changed over time (Figs. 6 to 9). Carbon stocks increased with MAP and decreased with MAT; these effects became stronger from past to present (Figs. 6A and 9, A and B). The effects of MAP and MAT on the net carbon sink were near zero in the past; however, from past to present, the effect of MAP became positive while the effect of MAT became negative (Figs. 6B and 9, C and D). Meanwhile, the positive effect of MAP and the negative effect of MAT on carbon gains increased over time (Figs. 6C and 9, E and F). The positive effect of MAP and the negative effect of MAT on carbon losses became weaker from past to present (Fig. 6D and 9, G and H). The only significant effect from soil variables was found for soil organic matter (SOM), which had negative effects on carbon gains and carbon losses (Fig. 6, C and D). Site area, which was used as a proxy of edge effects, has not displayed significant effects on the carbon dynamics variables (Fig. 6).

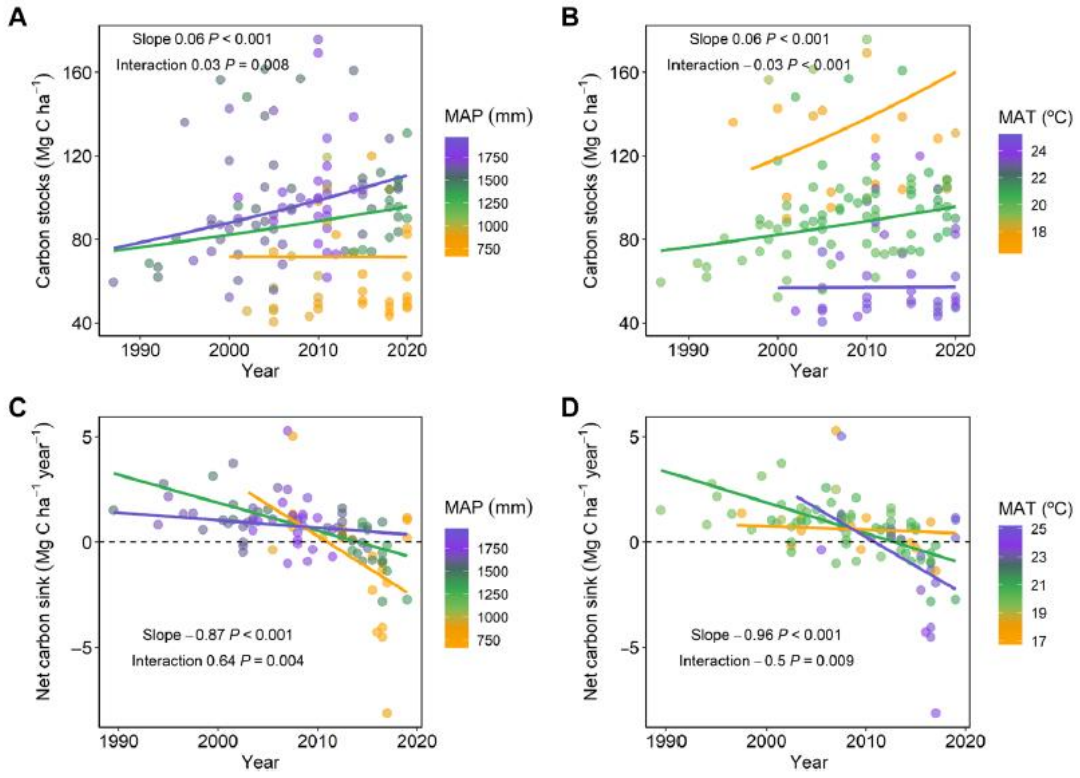

Fig. 7. Interaction effects between time and climate on carbon stocks and net carbon sink. (**A**) Carbon stocks, time as predictor and MAP as mediating variable. (**B**) Carbon stocks, time as predictor and MAT as mediating variable. (**C**) Net carbon sink, time as predictor and MAP as mediating variable. (**D**) Net carbon sink, time as predictor and MAT as mediating variable (best model containing MAT − ΔAICc = 4.02). In (A) and (B), censuses (n = 127) nested within sites (n = 32); in (C) and (D), census intervals (n = 95) nested within sites (n = 32). The coefficients were estimated by averaging the LMMs (including a random effect of site) with ΔAICc ≤ 4. Note that the slope of year of net carbon sink differs between (C) and (D) because the effects showed in (D) came from the best model containing MAT. The slopes and interactions of the carbon stock models were estimated in the logarithmic scale, and all models were fitted with scaled predictors.

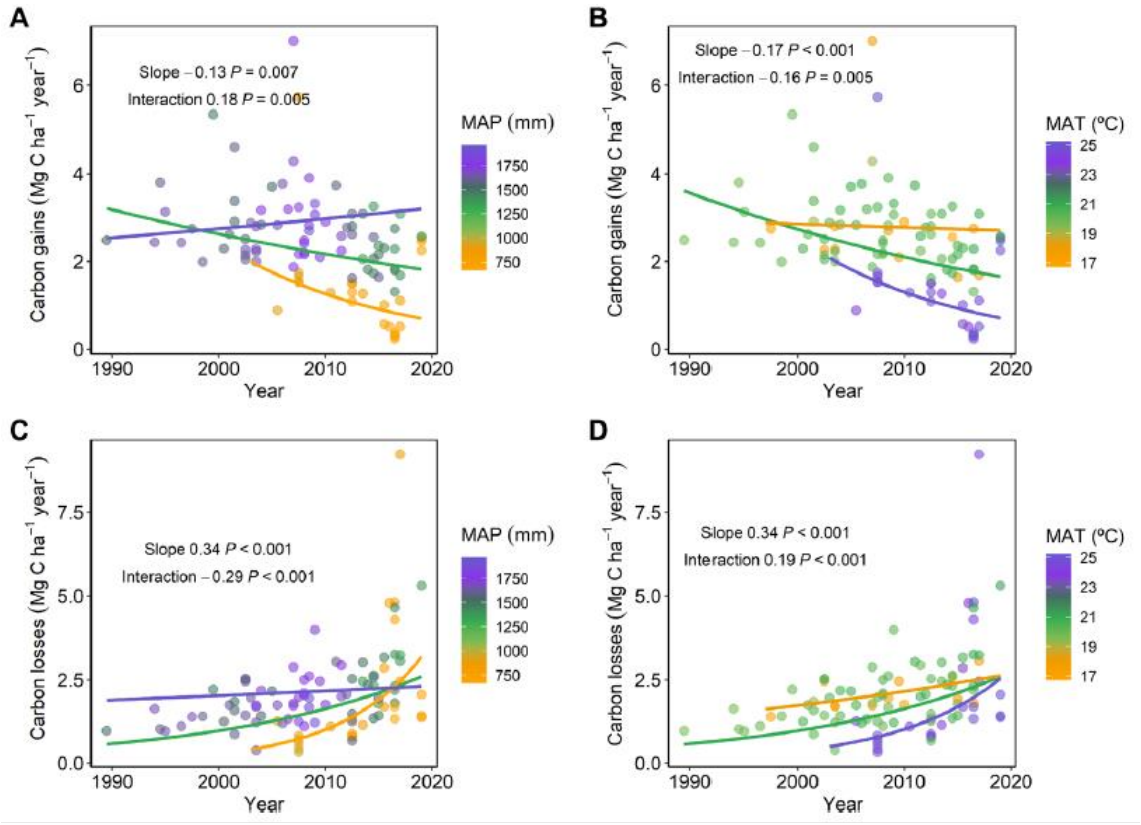

Fig. 8. Interaction effects between time and climate on carbon gains and carbon losses. (**A**) Carbon gains, time as predictor and MAP as mediating variable. (**B**) Carbon gains, time as predictor and MAT as mediating variable (best model containing MAT − ΔAICc = 12.2). (**C**) Carbon losses, time as predictor and MAP as mediating variable. (**D**) Carbon losses, time as predictor and MAT as mediating variable. Data with census intervals (n = 95) nested within sites (n = 32). The coefficients were estimated by averaging the LMMs (including a random effect of site) with ΔAICc ≤ 4. Note that the effect of year on carbon gains differs between (A) and (B) because the effects showed in (B) came from the best model containing MAT. The slopes and interactions were estimated in the logarithmic scale, and all models were fitted with scaled predictors.

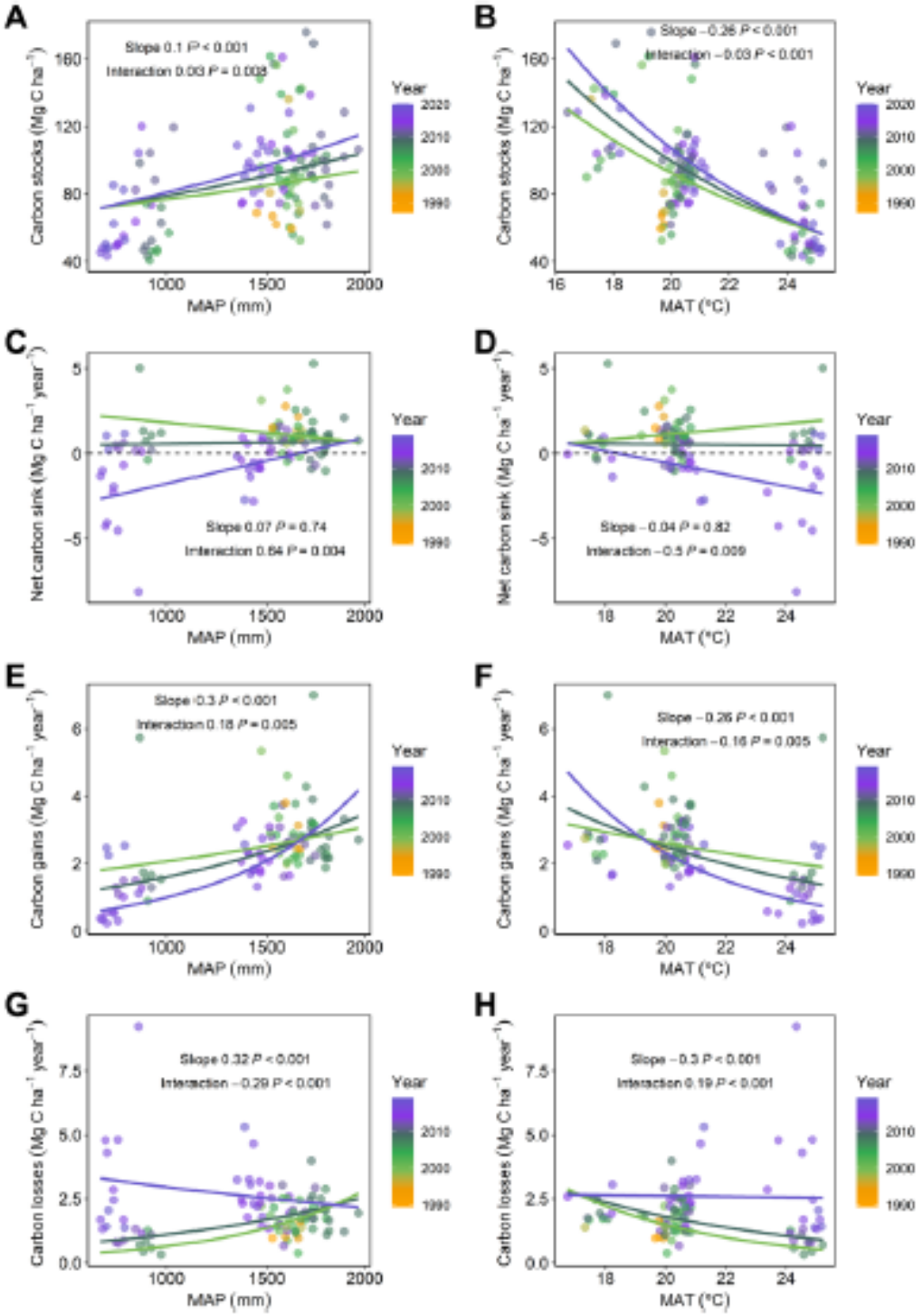

Fig. 9. Interaction effects between time and climate on carbon dynamics. (**A**) Carbon stocks, MAP as predictor and time as mediating variable. (**B**) Carbon stocks, MAT as predictor and time as mediating variable. (**C**) Net carbon sink, MAP as predictor and time as mediating variable. (**D**) Net carbon sink, MAT as predictor and time as mediating variable (best model containing MAT − ΔAICc = 4.02). (**E**) Carbon gains, MAP as predictor and time as mediating variable. (**F**) Carbon gains, MAT as predictor and time as mediating variable (best model containing MAT − ΔAICc = 12.2). (**G**) Carbon losses, MAP as predictor and time as mediating variable. (**H**) Carbon losses, MAT as predictor and time as mediating variable. In (A) and (B), censuses (n = 127) nested within sites (n = 32); in (C) to (H), census intervals (n = 95) nested within sites (n = 32). The coefficients were estimated by averaging the LMMs

(including a random effect of site) with $\Delta AICc \leq 4$. The slopes and interactions of the carbon stock, carbon gain, and carbon loss models were estimated in the logarithmic scale, and all models were fitted with scaled predictors.

DISCUSSION

The net carbon sink in southeastern Brazil's seasonal forests is declining over time by decreasing carbon gains and increasing carbon losses (Figs. 4 to 8). The carbon sink became a carbon source in 2013 (Fig. 4B), which explains the decline in carbon stocks after this year (Fig. 4A). Among the forests under different climates, the driest and warmest sites are experiencing the most severe decrease in carbon gains, the most severe increase in carbon losses, and, therefore, the most severe decline in the net carbon sink (Figs. 5 to 9). The severe decrease in the carbon sink of the driest and warmest forests suggests that these forests may have reached a climatic stress threshold (*9*). The carbon stocks of the driest and warmest sites remain stable with a slight (but nonsignificant) decrease (Figs. 5A and 7, A and B); however, if their net carbon sink remains in a negative balance, then their carbon stocks will also decline in the near future, as observed in the general trend after 2013 (Fig. 4A).

Under wet conditions, the carbon gains increased over time (Fig. 8A), consistent with the hypothesized pantropical increase in tree growth caused by CO2 fertilization (*6*, *18*, *24*). However, the long-term decrease in carbon gains experienced by the sites under intermediate climate and by the driest and warmest sites (Fig. 8, A and B) is inconsistent with CO2 fertilization effects and with findings in the Amazon forests (*6*, *18*, *24*). Recent evidence suggests that atmospheric CO2 increases are not necessarily translated into larger amounts of sequestered carbon by old-growth forest trees (*19*). A large portion of this CO2 surplus can be emitted back into the atmosphere by processes such as soil respiration (*19*). Alternative hypotheses might also explain this effect (*3*, *20*, *21*). High levels of CO2 can increase tree-to-tree competition by enhancing the growth of some species or individuals, which, at the stand level, can decrease carbon gains by constraining the growth of the suppressed trees (*5*, *21*). In addition, trees growing under increasing CO2 can acclimate to high CO2 availability, by reducing their photosynthetic capacity below the expected for a given CO2 level (*20*, *25*). The potential increases in liana density caused by increasing CO2 and decreasing MAP (Fig. 3, B and C) can also decrease carbon gains by stimulating tree-liana competition for light, water, and nutrients (*3*, *5*, *26–28*). Meanwhile, the potential direct effects of climate fluctuations, such as decreasing MAP and increasing MAT (Fig. 3, A and B), on carbon gains may have suppressed the effects of CO2 fertilization on photosynthesis and WUE. Because water is an important resource for photosynthesis and high temperatures enhance respiration, drought and rising temperatures can cause physiological stress (e.g., carbon starvation and hydraulic failure) and decrease tree growth (*5*, *6*, *22*, *29*, *30*).

The driest and warmest sites are experiencing the most severe increase in carbon losses over time (Fig. 5D and 8, C and D). This effect is possibly explained by the combined effects of increasing CO2, drought, and higher temperatures (Fig. 3) on tree mortality (*5*). Drought and high temperatures can directly drive tree mortality through physiological stress, which can be potentialized by the effects of CO2 on tree mortality (*5*, *31*, *32*). Increasing CO2 can accelerate the speed at which trees reach large heights, which would increase the rate at which they are exposed to dry upper canopy, lightning, and windthrow and to the physiological aspects associated with larger sizes (*5*, *33–35*). In addition, increases in liana density provoked by rising CO2 and drought can also enhance tree mortality by increasing tree-liana

competition for light and water (*3*, *5*, *26–28*). The decrease in carbon gains and the increase in carbon losses of the driest and warmest sites over time, which have a distinct flora, naturally associated with dry and warm conditions, suggest that these forests may have reached a stress threshold due to the effects of increasing drought, temperature, and CO2 (*5*, *9*).

Carbon stocks and carbon gains decreased with MAT and increased with MAP over space (Fig. 9, A and B, and E and F), as expected by theory (*6*, *29*, *36*). These effects are evidence of the physiological responses to the harsh conditions imposed by high temperatures and drought, which are related to physiological stress (*5*, *6*, *29*). However, the wettest and coldest sites have both greater carbon gains and greater carbon losses (Fig. 9, E to H), consistent with the high-gain high-loss dynamic pattern (*6*). Therefore, the spatial effects of MAT and MAP on the net carbon sink were near zero most of time and became negative for MAT and positive for MAP from past to present (Fig. 9, C and D). These shifts in the spatial effects of climate occurred because the driest and warmest sites experienced the most severe increase in their carbon losses and the most severe decrease in their carbon gains over time. Thus, the net carbon sink of the driest and warmest sites became smaller than the net carbon sink of the wettest and coldest sites. Although MAT was more important than MAP to differentiate the forest types (fig. S3), MAP was more important than MAT to predict the net carbon sink, carbon gains, and carbon losses (Fig. 6). Soil variables were important to differentiate forest types (figs. S3 and S4); however, only SOM displayed significant effects on carbon dynamics. Forests on soils with lower levels of SOM tend to have higher carbon gains and higher carbon losses (Fig. 6, C and D). SOM is related to soil quality and higher productivity; thus, these effects are not conclusive and should be further investigated. In addition, site area, which was a proxy of edge effects, has not displayed significant effects in the carbon dynamics (Fig. 6). Therefore, the results suggest that climate is the most important predictor of the spatial patterns of carbon dynamics in our study region.

We recognize the limitations of our data, such as space-for-time (sites with only one census interval; table S1) and unbalanced spatial-temporal sampling efforts (Fig. 2 and figs. S1 and S2). However, the negative trend and the negative balance of the carbon sink were a clear pattern in our data and results. In general, these forests are shifting from carbon sinks to carbon sources. Currently, the forests under intermediate climate conditions and the forests under the driest and warmest conditions are already carbon sources, probably because they may have reached a stress threshold. Meanwhile, the carbon sink of the wettest and coldest forests is continually declining. The driest and warmest forests naturally have lower carbon stocks (Fig. 9, A and B), which will decline in the near future if their net carbon sink remains in a negative balance. These long-term trends in carbon dynamics are likely to be influenced by climate fluctuations and rising CO2 (*5*, *6*, *22*). However, because these factors are correlated and can interact over time, their mechanistic individual effects and the effects of other unmeasured drivers remain uncertain and should be further investigated. Atmospheric CO2 concentration, temperature, and drought events are expected to continue increasing in upcoming decades, implying that the ecosystem functioning of southeastern Brazil tropical seasonal forests may be under threat (*5*, *6*, *9*).

Political actions to mitigate greenhouse gas emissions, together with conservation policies to protect these ecosystems, are needed. We also argue that the driest and warmest sites (deciduous forests, SDTFs) should be further included in conservation policies and that revegetation strategies in agricultural areas can be useful to offset the decline in the carbon sink and stocks. Beyond the political implications, our findings are also useful to improve the

predictions of future global carbon sink and to bring knowledge to the carbon cycle of tropical forests.

MATERIALS AND METHODS

Study design

We used tree community data from 32 repeatedly measured permanent forest sites located in southeastern Brazil (Fig. 1). The greatest distances among sites are 900 km (latitude) and 177 km (longitude) (Fig. 1); sites' altitudes range between 450 and 1475 m above sea level (mean, 898 m); MAP is between 666.4 and 1967.3 mm (mean, 1409.2 mm) (Fig. 2A); MAT is between 16.7° and 25.2°C (mean, 21.1°C) (Fig. 2A); and site area is between 3 and 1200 ha (mean, 78 ha). Our data comprise 95 census intervals (nested within 32 sites), the first census in our dataset was in 1987, and the most recent was in 2020 (table S1). The sites encompass three forest types: deciduous forests (the driest and warmest sites; flat topography; >50% of the individuals lose their leaves in the dry season; 24 census intervals nested within 11 sites; monitored from 2002 to 2020), evergreen forests (the wettest and coldest sites; undulating topography; no deciduousness; 12 census intervals nested within 5 sites; monitored from 1995 to 2020), and semideciduous forests (intermediate climate; undulating topography; 20 to 50% of the individuals lose their leaves in the dry season; 59 census intervals nested within 16 sites; monitored from 1987 to 2020) (table S1). The soils of the deciduous forests have higher levels of phosphorus and cation exchange capacity (CEC) (figs. S3 and S4). All sites are closed canopy forests, in advanced successional stages, free from fire, flood, landslides, and human disturbances at least for the decades preceding the first census of each site. The historical record is based on personal communication with the local people, land owners, or reserve managers. In addition to the historical records, field observations also corroborate the absence of human disturbances, fire, flood, and landslides during the monitoring time. There is no record of wind disturbances, although wind effects cannot be disregarded. Because all sites are in advanced successional stages, there are no differences in the successional stages between forest types (figs. S5 to S22). The diametric structure and diversity distribution over diameter classes are very similar among sites and forest types (figs. S5 to S20) and no significant differences in the community weighted means of wood density (WD) (details on WD below) between forest types were detected (figs. S21 and S22). Sampling (sampled area) was designed to capture Intra-site heterogeneity (most subplots are located in the interior of the sites, but edges were also captured by the samples) and spanned from 0.2 to 5 ha (mean of 1.05 ha) (using subplots of 400 m2, 20 m by 20 m, in most cases) in each study site, totaling 33.5 ha (Fig. 2B, fig. S1, and table S1). The sampled plots were measured at least twice in every site (table S1). The number of censuses per site varied between two and eight (mean five censuses per site), and census interval length varied among sites and within the same site over time, ranging from 1 to 9 years (mean, 5 years) (table S1). The total monitoring length per site varied from 5 to 31 years (mean, 15 years) (Fig. 2C and fig. S2). Forest inventory data are hosted in the ForestPlots.net system (www.forestplots.net).

All trees with quadratic mean diameter at reference height (1.3 m) [diameter at breast height (DBH)] ≥5 cm were measured in each census (*37*). This inclusion criterion allows to include tree individuals with multiple stems (stems with DBH ≤ 5 cm) if the quadratic mean diameter at reference height of the tree individual meets the criterion. The height of the point of measurement (POM) was marked in the stems and used as a reference for subsequent measures. When changing the POM was necessary for a given stem, its diameter growth was estimated using a ratio between the current and previous POMs (*38*). Plant identification

followed Angiosperm Phylogeny Group IV (*39*) and was performed by experts in the field or by consulting herbaria, and species names were standardized using Flora do Brasil 2020 (http://reflora.jbrj.gov.br/reflora/floradobrasil). To obtain WD values, the species were matched to the global WD database (*40*). When WD was not available at the species level, the average WD of other species from the same genus or family was used.

The aboveground woody biomass (AGWB) of each tree was obtained with the modified pantropical allometric equation of Chave *et al.* (*41*) (Eq. 1) through the BIOMASS R package (*42*). We used the equation with the parameters for tree diameter, WD, and environmental stress (E) because tree height data are absent in our censuses. Equation 1 is broadly applied to tropical forests worldwide for deriving from a large dataset encompassing the pantropical region of the globe. But another equation (Eq. 2), proposed by Sampaio and Silva (*43*), was developed specifically to estimate tree aboveground biomass of deciduous tropical forests in the Brazilian Caatinga domain, which is the case for the deciduous forests of our dataset. Therefore, to reduce the uncertainty in the biomass estimates of the deciduous forests, we combined (averaged) the estimated values of Eqs. 1 and 2 for deciduous forest trees. The correlation between the estimated values of the two equations is 0.81 (Pearson correlation), but the mean of the estimated values from Eq. 1 was 2.2% greater than the estimated values from Eq. 2. The AGWB was converted to aboveground carbon (AGC) assuming that AGC is 45.6% of the AGWB (*44*). We estimated the carbon stock (Mg C ha−1) of each site in each census as the sum of each living tree's AGC, scaled to hectares. Carbon gains (Mg C ha−1 year−1) were estimated as the sum of the growth of the surviving trees (tree AGC at the end of the interval minus the tree AGC at the start of the interval) plus the sum of the AGC of the recruited trees (tree individuals or stems that reached DBH ≥ 5 cm at the end of the interval, assuming DBH = 0 at the start of the interval). The sum of the growth of the survivors with the AGC of the recruited trees was divided by the interval length (in years) and then scaled to hectares. Carbon losses (Mg C ha−1 year−1) were estimated as the sum of the AGC of the individuals and stems that died during a census interval, divided by the census interval length (in years), and then scaled to hectares. As carbon gains and losses are biased by census interval length, we corrected their values using the equation *CIC*1 proposed by Talbot *et al.* (*38*). We calculated net carbon sink (Mg C ha−1 year−1) as carbon gains minus carbon losses. Note that the length of each census interval was calculated using the rounded years (i.e., year of the end of the interval minus the year of the start of the interval).

$$\mathrm{AGB\ (Mg\ )} = \exp(-2.024 - 0.896 \times \mathrm{E} + 0.920 \times \ln(\mathrm{WD\ }) + 2.795 \times \ln(\mathrm{DBH\ }) - 0.0461 \times (\ln(\mathrm{DBH})\ 2\ )\ ) \quad (1)$$

and

$$\mathrm{AGB\ (kg\ )} = 0.1730 \times \mathrm{DBH}\ 2.295 \quad (2)$$

where DBH is the diameter at breast height (cm), WD is the wood density (g cm−3), and E is the environmental stress.

Climate data

We obtained monthly mean temperature (°C), monthly average daily maximum temperature (°C), monthly precipitation (mm), and daily potential evapotranspiration (PET; mm) from the Climatic Research Unit (CRU TS version 4.04, released 24 April 2020; https://crudata.uea.ac.uk/cru/data/hrg) (*45*). We used data from WorldClim 2.1 (*46*) to

downscale the CRU temperature and precipitation data to 1 km2 and then applied the monthly correction for all months in each census interval. Delta spatial downscaling method was used for downscaling; see Peng *et al.* (*47*) for details. We calculated annual maximum climatological water deficit (CWD) by summing the differences between monthly downscaled precipitation (mP) and monthly PET (PET minus mP) only when this difference was positive (i.e., evapotranspiration exceeded precipitation: water deficit). We used the average values of MAT, maximum temperature (max temp), CWD, and MAP of the years within each census interval. For the sites measured in 2020, for which climate data were not available in CRU TS version 4.04, we used climate data ranging from the start of the interval to the end of 2019. The climate space and the temporal trends can be found in Figs. 2A and 3 (A and B). Note that for the first census of the census level data (carbon stocks), we used the averaged climate values from 5 years before the first census of each site. Max temp is strongly correlated with MAT ($r = 0.99$) and MAP is strongly correlated with CWD ($r = -0.96$); thus, we opted to use MAT and MAP because these variables are easier to obtain and are usually more accessible than max temp and CWD.

Atmospheric CO2 concentration

We used annual mean values of atmospheric CO2 (ppm) concentration from the Mauna Loa record (*48*). We also calculated the rate of CO2 change (ppm year−1) by subtracting the CO2 concentration at the end of the interval by the CO2 concentration at the start of the interval and then dividing this difference by the census interval length. Both CO2 concentration and CO2 change increased over time (Fig. 3C and figs. S23 and S24). The Pearson correlation between CO2 concentration and year is 0.99 while between CO2 change and year the correlation is 0.85. Therefore, we opted to use time (year) in the models instead of CO2 variables. We did this because the potential effects of CO2 are not distinguishable from the effects of other environmental variables over time, such as climate fluctuations and other unmeasured potential predictors.

Soil data

To control the potential effects of soil, we collected soil surface samples (20 cm of depth) in the first census of each site. Soil surface samples were collected from three points in each subplot and later combined into one composite sample. Following the protocol by the Empresa Brasileira de Pesquisa Agropecuaria (*49*), the following soil attributes were obtained: pH in water (pH), phosphorus (mg cm−3) (P), potassium (mg × cm−3) (K), calcium (cmolc × dm−3) (Ca), magnesium (cmolc × dm−3) (Mg), aluminum (cmolc × dm−3) (Al), sum of bases (SB) (cmolc × dm−3), cation exchange capacity (cmolc × dm−3) (CEC), soil organic matter (dag × kg−1) (SOM), and clay percentage (%) (clay). We calculated the mean of each soil variable for each site.

Statistical analysis

All analyses were carried out in the R environment version 3.6.1 (*50*). Because of the nonindependence between observations within the same site (temporal autocorrelation; repeated measurements in the same sites over time), our modeling and statistical framework were based on tools that control for the nonindependence between observations. We used generalized additive models (GAMs) with a random effect of site and linear mixed-effects models (LMMs), which allow the intercepts to vary randomly among sites. We used the mgcv

package (*51*) to fit the GAMs and the lme4 package (*52*) to fit the LMMs. We did not include random slopes because some sites have few census intervals, preventing the models to achieve convergence. All models were fitted under normality assumptions (Gaussian family). We assessed residual normality and homoscedasticity through residual inspection. We applied logarithmic transformation on carbon stocks, carbon gains, and carbon losses to meet normality assumptions. As plots vary in spatial and temporal sampling efforts (Fig. 2), we weighted the observations (prior weights) by sampled area and census interval length. For carbon stock models, we weighted by the cubic root of the sampled area (*36*), and for the other response variables, we weighted by the cubic root of census interval length plus the fourth root of sampled area minus one (*6*).

The modeling framework can be divided into three parts: (i) the general long-term trends of carbon dynamics (carbon stocks, net carbon sink, carbon gains, and carbon losses), (ii) the long-term trends of carbon dynamics by forest type, and (iii) a final model including time (as a proxy of the effects of rising CO2, climate fluctuations, and other unmeasured confounding effects over time), climate and soil, and the interactions between time and climate. The interactions between climate and time allowed to evaluate whether sites under different climate conditions differ in their long-term trends and whether the effects of climate have changed over time. Note that we have not included climate and forest type in the same model because forest type is correlated with climate and soil (Fig. 2 and figs. S3 and S4), leading to high variance inflation factor (VIF) values when they are in the same model. We used GAMs only in part 1 because we do not have sufficient data to fit the models of parts 2 and 3 with smoothing splines (overfitting). In all models, we used the year corresponding to the midpoint of each census interval (except for carbon stock model, to which we used census year).

To estimate the long-term trends of carbon dynamics variables (bivariate relationships) (part 1), we used GAMs and LMMs. More specifically, we regressed the carbon dynamics variables as function of time (year). We estimated the long-term trends of each forest type using LMM (part 2). Because of the strong multicollinearity between the environmental variables, before building the global model of part 3, we removed collinear variables to avoid redundant and circular interpretations. In general, we removed variables with Pearson correlation ($r \geq |0.75|$), with the following exceptions: Although strongly correlated ($r \geq |0.75|$), we maintained MAP and MAT ($r = -0.89$), and CEC as a proxy of soil fertility (which is strongly correlated with climate) (see correlation matrix at fig. S24 for details). We also controlled for the potential effects of site area (proxy of edge effects) by including the area of the site (site area) in the global model. Thus, the final set of variables included in the global model was year, MAP, MAT, P, CEC, SOM, clay, and site area. The global model was built in a way that the independent effect of each explanatory variable was accounted, as well as the interactions between year with MAP and MAT (Eq. 3). All predictors were scaled and centered to zero mean and unit variance. In addition, we checked for spatial autocorrelation in global models' residuals using Moran's I test, implemented in package ncf (*53*).

$$\text{Carbon dynamics} \sim \text{year} \times (\text{MAT} + \text{MAP}) + \text{P} + \text{CEC} + \text{SOM} + \text{clay} + \text{site area} \quad (3)$$

where carbon dynamics is carbon stocks, net carbon sink, carbon gains, and carbon losses. Additive and interaction effects are represented, respectively, by "+" and "×." Note that the independent effects of year, MAT, and MAP are included in the interaction term.

An information theoretical approach based on the Akaike Information Criterion of second order (AICc) was used for model selection (*54*). From the global model (Eq. 1) of each response variable, we obtained the set of best models (those with ΔAICc ≤ 4) (*54*). To avoid multicollinearity issues, the selected models were constrained to have explanatory variables with $r \geq |0.6|$ (*55*), ensuring low VIF values (VIF ≤ 4). To avoid overfitting, we also limited the best models' degrees of freedom, ensuring at least 15 observations per term. Using multimodel inference, we averaged the coefficients of the selected models and used the conditional averaged coefficients as a final result (*54*). The relative importance of the predictors was not considered, given that some variables were not contained in the same number of models because of collinearity, which could bias the sum of Akaike weights (*54*). Our conclusions relied on the significant conditional averaged coefficients (significance level of 0.05). The MuMIn package (*56*) was used for model selection, model averaging, and to obtain the marginal $R2$ (variance explained by the fixed effects, we used the average between the marginal $R2$ of the best model and the marginal $R2$ of the global model) (*57*). Graphics were obtained through the packages ggplot2, viridis, and corrplot (*58–60*).

REFERENCES AND NOTES

1. C. Beer, M. Reichstein, E. Tomelleri, P. Ciais, M. Jung, N. Carvalhais, C. Rodenbeck, M. A. Arain, D. Baldocchi, G. B. Bonan, A. Bondeau, A. Cescatti, G. Lasslop, A. Lindroth, M. Lomas, S. Luyssaert, H. Margolis, K. W. Oleson, O. Roupsard, E. Veenendaal, N. Viovy, C. Williams, F. I. Woodward, D. Papale, Terrestrial gross carbon dioxide uptake: Global distribution and covariation with climate. *Science* **329**, 834–838 (2010).

2. Y. Pan, R. A. Birdsey, O. L. Phillips, R. B. Jackson, The structure, distribution, and biomass of the World's Forests. *Annu. Rev. Ecol. Evol. Syst.* **44**, 593–622 (2013).

3. K. J. Feeley, S. Joseph Wright, M. N. Nur Supardi, A. R. Kassim, S. J. Davies, Decelerating growth in tropical forest trees. *Ecol. Lett.* **10**, 461–469 (2007).

4. D. Li, S. Wu, L. Liu, Y. Zhang, S. Li, Vulnerability of the global terrestrial ecosystems to climate change. *Glob. Chang. Biol.* **24**, 4095–4106 (2018).

5. N. McDowell, C. D. Allen, K. Anderson-Teixeira, P. Brando, R. Brienen, J. Chambers, B. Christoffersen, S. Davies, C. Doughty, A. Duque, F. Espirito-Santo, R. Fisher, C. G. Fontes, D. Galbraith, D. Goodsman, C. Grossiord, H. Hartmann, J. Holm, D. J. Johnson, A. R. Kassim, M. Keller, C. Koven, L. Kueppers, T. Kumagai, Y. Malhi, S. M. McMahon, M. Mencuccini, P. Meir, P. Moorcroft, H. C. Muller-Landau, O. L. Phillips, T. Powell, C. A. Sierra, J. Sperry, J. Warren, C. Xu, X. Xu, Drivers and mechanisms of tree mortality in moist tropical forests. *New Phytol.* **219**, 851–869 (2018).

6. W. Hubau, S. L. Lewis, O. L. Phillips, K. Affum-Baffoe, H. Beeckman, A. Cuni-Sanchez, A. K. Daniels, C. E. N. Ewango, S. Fauset, J. M. Mukinzi, D. Sheil, B. Sonke, M. J. P. Sullivan, T. C. H. Sunderland, H. Taedoumg, S. C. Thomas, L. J. T. White, K. A. Abernethy, S. Adu-Bredu, C. A. Amani, T. R. Baker, L. F. Banin, F. Baya, S. K. Begne, A. C. Bennett, F. Benedet, R. Bitariho, Y. E. Bocko, P. Boeckx, P. Boundja, R. J. W. Brienen, T. Brncic, E. Chezeaux, G. B. Chuyong, C. J. Clark, M. Collins, J. A. Comiskey, D. A. Coomes, G. C. Dargie, T. de Haulleville, M. N. D. Kamdem, J.-L. Doucet, A. Esquivel-Muelbert, T. R. Feldpausch, A. Fofanah, E. G. Foli, M. Gilpin, E. Gloor, C. Gonmadje, S. Gourlet-Fleury,

J. S. Hall, A. C. Hamilton, D. J. Harris, T. B. Hart, M. B. N. Hockemba, A. Hladik, S. A. Ifo, K. J. Jeffery, T. Jucker, E. K. Yakusu, E. Kearsley, D. Kenfack, A. Koch, M. E. Leal, A. Levesley, J. A. Lindsell, J. Lisingo, G. Lopez-Gonzalez, J. C. Lovett, J.-R. Makana, Y. Malhi, A. R. Marshall, J. Martin, E. H. Martin, F. M. Mbayu, V. P. Medjibe, V. Mihindou, E. T. A. Mitchard, S. Moore, P. K. T. Munishi, N. N. Bengone, L. Ojo, F. E. Ondo, K. S.-H. Peh, G. C. Pickavance, A. D. Poulsen, J. R. Poulsen, L. Qie, J. Reitsma, F. Rovero, M. D. Swaine, J. Talbot, J. Taplin, D. M. Taylor, D. W. Thomas, B. Toirambe, J. T. Mukendi, D. Tuagben, P. M. Umunay, G. M. F. van der Heijden, H. Verbeeck, J. Vleminckx, S. Willcock, H. Woll, J. T. Woods, L. Zemagho, Asynchronous carbon sink saturation in African and Amazonian tropical forests. *Nature* **579**, 80–87 (2020).

7. E. T. A. Mitchard, The tropical forest carbon cycle and climate change. *Nature* **559**, 527–534 (2018).

8. X. Feng, M. Uriarte, G. Gonzalez, S. Reed, J. Thompson, J. K. Zimmerman, L. Murphy, Improving predictions of tropical forest response to climate change through integration of field studies and ecosystem modeling. *Glob. Chang. Biol.* **24**, e213–e232 (2018).

9. K. Allen, J. M. Dupuy, M. G. Gei, C. Hulshof, D. Medvigy, C. Pizano, B. Salgado-Negret, C. M. Smith, A. Trierweiler, S. J. Van Bloem, B. G. Waring, X. Xu, J. S. Powers, Will seasonally dry tropical forests be sensitive or resistant to future changes in rainfall regimes? *Environ.Res. Lett.* **12**, 023001 (2017).

10. A. D. A. Castanho, M. T. Coe, P. Brando, M. Macedo, A. Baccini, W. Walker, E. M. Andrade, Potential shifts in the aboveground biomass and physiognomy of a seasonally dry tropical forest in a changing climate. *Environ. Res. Lett.* **15**, 034053 (2020).

11. D. J. Zarin, N. L. Harris, A. Baccini, D. Aksenov, M. C. Hansen, C. Azevedo-Ramos, T. Azevedo, B. A. Margono, A. C. Alencar, C. Gabris, A. Allegretti, P. Potapov, M. Farina, W. S. Walker, V. S. Shevade, T. V. Loboda, S. Turubanova, A. Tyukavina, Can carbon emissions from tropical deforestation drop by 50% in 5 years? *Glob. Chang. Biol.* **22**, 1336–1347 (2016).

12. C. A. Portillo-Quintero, G. A. Sanchez-Azofeifa, Extent and conservation of tropical dry forests in the Americas. *Biol. Conserv.* **143**, 144–155 (2010).

13. D. Schimel, B. B. Stephens, J. B. Fisher, Effect of increasing CO2 on the terrestrial carbon cycle. *Proc. Natl. Acad. Sci. U.S.A.* **112**, 436–441 (2015).

14. C. Quere, R. Andrew, P. Friedlingstein, S. Sitch, J. Hauck, J. Pongratz, P. Pickers, J. Ivar Korsbakken, G. Peters, J. Canadell, A. Arneth, V. Arora, L. Barbero, A. Bastos, L. Bopp, P. Ciais, L. Chini, P. Ciais, S. Doney, T. Gkritzalis, D. Goll, I. Harris, V. Haverd, F. Hoffman, M. Hoppema, R. Houghton, G. Hurtt, T. Ilyina, A. Jain, T. Johannessen, C. Jones, E. Kato, R. Keeling, K. Klein Goldewijk, P. Landschutzer, N. Lefevre, S. Lienert, Z. Liu, D. Lombardozzi, N. Metzl, D. Munro, J. Nabel, S. I. Nakaoka, C. Neill, A. Olsen, T. Ono, P. Patra, A. Peregon, W. Peters, P. Peylin, B. Pfeil, D. Pierrot, B. Poulter, G. Rehder, L. Resplandy, E. Robertson, M. Rocher, C. Rodenbeck, U. Schuster, I. Skjelvan, R. Seferian, I. Skjelvan, T. Steinhoff, A. Sutton, P. Tans, H. Tian, B. Tilbrook, F. Tubiello, I. Van Der Laan-Luijkx, G. van der Werf, N. Viovy, A. Walker, A. Wiltshire, R. Wright, S. Zaehle, B. Zheng, Global Carbon Budget 2018. *Earth Syst. Sci. Data.* **10**, 2141–2194 (2018).

15. A. Robredo, U. Perez-Lopez, H. Sainz De La Maza, B. Gonzalez-Moro, M. Lacuesta, A. Mena-Petite, A. Munoz-Rueda, Elevated CO2 alleviates the impact of drought on barley improving water status by lowering stomatal conductance and delaying its effects on photosynthesis. *Environ. Exp. Bot.* **59**, 252–263 (2007).

16. J. A. M. Holtum, K. Winter, Elevated [CO2] and forest vegetation: More a water issue than a carbon issue? *Funct. Plant Biol.* **37**, 694–702 (2010).

17. S. Piao, S. Sitch, P. Ciais, P. Friedlingstein, P. Peylin, X. Wang, A. Ahlstrom, A. Anav, J. G. Canadell, N. Cong, C. Huntingford, M. Jung, S. Levis, P. E. Levy, J. Li, X. Lin, M. R. Lomas, M. Lu, Y. Luo, Y. Ma, R. B. Myneni, B. Poulter, Z. Sun, T. Wang, N. Viovy, S. Zaehle, N. Zeng, Evaluation of terrestrial carbon cycle models for their response to climate variability and to CO2 trends. *Glob. Chang. Biol.* **19**, 2117–2132 (2013).

18. C. Huntingford, P. Zelazowski, D. Galbraith, L. M. Mercado, S. Sitch, R. Fisher, M. Lomas, A. P. Walker, C. D. Jones, B. B. B. Booth, Y. Malhi, D. Hemming, G. Kay, P. Good, S. L. Lewis, O. L. Phillips, O. K. Atkin, J. Lloyd, E. Gloor, J. Zaragoza-Castells, P. Meir, R. Betts, P. P. Harris, C. Nobre, J. Marengo, P. M. Cox, Simulated resilience of tropical rainforests to CO2-induced climate change. *Nat. Geosci.* **6**, 268–273 (2013).

19. M. Jiang, B. E. Medlyn, J. E. Drake, R. A. Duursma, I. C. Anderson, C. V. M. Barton, M. M. Boer, Y. Carrillo, L. Castaneda-Gomez, L. Collins, K. Y. Crous, M. G. De Kauwe, B. M. dos Santos, K. M. Emmerson, S. L. Facey, A. N. Gherlenda, T. E. Gimeno, S. Hasegawa, S. N. Johnson, A. Kannaste, C. A. Macdonald, K. Mahmud, B. D. Moore, L. Nazaries, E. H. J. Neilson, U. N. Nielsen, U. Niinemets, N. J. Noh, R. Ochoa-Hueso, V. S. Pathare, E. Pendall, J. Pihlblad, J. Pineiro, J. R. Powell, S. A. Power, P. B. Reich, A. A. Renchon, M. Riegler, R. Rinnan, P. D. Rymer, R. L. Salomon, B. K. Singh, B. Smith, M. G. Tjoelker, J. K. M. Walker, A. Wujeska-Klause, J. Yang, S. Zaehle, D. S. Ellsworth, The fate of carbon in a mature forest under carbon dioxide enrichment. *Nature* **580**, 227–231 (2020).

20. J. Penuelas, J. G. Canadell, R. Ogaya, Increased water-use efficiency during the 20th century did not translate into enhanced tree growth. *Glob. Ecol. Biogeogr.* **20**, 597–608 (2011).

21. L. Fernandez-de-Una, N. G. Mcdowell, I. Canellas, G. Gea-Izquierdo, Disentangling the effect of competition, CO2 and climate on intrinsic water-use efficiency and tree growth. *J. Ecol.* **104**, 678–690 (2016).

22. R. J. W. Brienen, O. L. Phillips, T. R. Feldpausch, E. Gloor, T. R. Baker, J. Lloyd, G. Lopez-Gonzalez, A. Monteagudo-Mendoza, Y. Malhi, S. L. Lewis, R. Vasquez Martinez, M. Alexiades, E. Alvarez Davila, P. Alvarez-Loayza, A. Andrade, L. E. O. C. Aragao, A. Araujo-Murakami, E. J. M. M. Arets, L. Arroyo, G. A. Aymard, C. O. S. Banki, C. Baraloto, J. Barroso, D. Bonal, R. G. A. Boot, J. L. C. Camargo, C. V. Castilho, V. Chama, K. J. Chao, J. Chave, J. A. Comiskey, F. C. Valverde, L. Da Costa, E. A. De Oliveira, A. Di Fiore, T. L. Erwin, S. Fauset, M. Forsthofer, D. R. Galbraith, E. S. Grahame, N. Groot, B. Herault, N. Higuchi, E. N. Honorio Coronado, H. Keeling, T. J. Killeen, W. F. Laurance, S. Laurance, J. Licona, W. E. Magnussen, B. S. Marimon, B. H. Marimon-Junior, C. Mendoza, D. A. Neill, E. M. Nogueira, P. Nunez, N. C. Pallqui Camacho, A. Parada, G. Pardo-Molina, J. Peacock, M. Pena-Claros, G. C. Pickavance, N. C. A. Pitman, L. Poorter, A. Prieto, C. A. Quesada, F.

Ramirez, H. Ramirez-Angulo, Z. Restrepo, A. Roopsind, A. Rudas, R. P. Salomao, M. Schwarz, N. Silva, J. E. Silva-Espejo, M. Silveira, J. Stropp, J. Talbot, H. Ter Steege, J. Teran-Aguilar, J. Terborgh, R. Thomas-Caesar, M. Toledo, M. Torello-Raventos, R. K. Umetsu, G. M. F. van der Heijden, P. van der Hout, I. C. Guimaraes Vieira, S. A. Vieira, E. Vilanova, V. A. Vos, R. J. Zagt, Long-term decline of the Amazon carbon sink. *Nature* **519**, 344–348 (2015).

23. Y. Yang, H. Guan, O. Batelaan, T. R. McVicar, D. Long, S. Piao, W. Liang, B. Liu, Z. Jin, C. T. Simmons, Contrasting responses of water use efficiency to drought across global terrestrial ecosystems. *Sci. Rep.* **6**, 23284 (2016).

24. S. L. Lewis, Y. Malhi, O. L. Phillips, Fingerprinting the impacts of global change on tropical forests. *Philos. Trans. R. Soc. Lond. B Biol. Sci.* **359**, 437–462 (2004).

25. S. P. Long, E. A. Ainsworth, A. Rogers, D. R. Ort, Rising atmospheric carbon dioxide: Plants FACE the future. *Annu. Rev. Plant Biol.* **55**, 591–628 (2004).

26. J. Granados, C. Korner, In deep shade, elevated CO2 increases the vigor of tropical climbing plants. *Glob. Chang. Biol.* **8**, 1109–1117 (2002).

27. S. J. DeWalt, S. A. Schnitzer, J. Chave, F. Bongers, R. J. Burnham, Z. Cai, G. Chuyong, D. B. Clark, C. E. N. Ewango, J. J. Gerwing, E. Gortaire, T. Hart, G. Ibarra-Manriquez, K. Ickes, D. Kenfack, M. J. Macia, J.-R. Makana, M. Martinez-Ramos, J. Mascaro, S. Moses, H. C. Muller-Landau, M. P. E. Parren, N. Parthasarathy, D. R. Perez-Salicrup, F. E. Putz, H. Romero-Saltos, D. Thomas, Annual rainfall and seasonality predict pan-tropical patterns of liana density and basal area. *Biotropica* **42**, 309–317 (2010).

28. S. A. Schnitzer, Increasing liana abundance in neotropical forests: Causes and consequences. *Ecol. Lianas* **2014**, 451–464 (2014).

29. D. A. Clark, S. C. Piper, C. D. Keeling, D. B. Clark, Tropical rain forest tree growth and atmospheric carbon dynamics linked to interannual temperature variation during 1984–2000. *Proc. Natl. Acad. Sci. U.S.A.* **100**, 5852–5857 (2003).

30. P. G. Taylor, C. C. Cleveland, W. R. Wieder, B. W. Sullivan, C. E. Doughty, S. Z. Dobrowski, A. R. Townsend, Temperature and rainfall interact to control carbon cycling in tropical forests. *Ecol. Lett.* **20**, 779–788 (2017).

31. O. L. Phillips, G. van der Heijden, S. L. Lewis, G. Lopez-Gonzalez, L. E. O. C. Aragao, J. Lloyd, Y. Malhi, A. Monteagudo, S. Almeida, E. A. Davila, I. Amaral, S. Andelman, A. Andrade, L. Arroyo, G. Aymard, T. R. Baker, L. Blanc, D. Bonal, A. C. A. de Oliveira, K.-J. Chao, N. D. Cardozo, L. da Costa, T. R. Feldpausch, J. B. Fisher, N. M. Fyllas, M. A. Freitas, D. Galbraith, E. Gloor, N. Higuchi, E. Honorio, E. Jimenez, H. Keeling, T. J. Killeen, J. C. Lovett, P. Meir, C. Mendoza, A. Morel, P. N. Vargas, S. Patino, K. S.-H. Peh, A. P. Cruz, A. Prieto, C. A. Quesada, F. Ramirez, H. Ramirez, A. Rudas, R. Salamao, M. Schwarz, J. Silva, M. Silveira, J. W. F. Slik, B. Sonke, A. S. Thomas, J. Stropp, J. R. D. Taplin, R. Vasquez, E. Vilanova, Drought–mortality relationships for tropical forests Oliver. *New Phytol.* **187**, 631–646 (2010).

32. M. O. Johnson, D. Galbraith, M. Gloor, H. De Deurwaerder, M. Guimberteau, A. Rammig, K. Thonicke, H. Verbeeck, C. von Randow, A. Monteagudo, O. L. Phillips, R. J. W. Brienen, T. R. Feldpausch, G. L. Gonzalez, S. Fauset, C. A. Quesada, B. Christoffersen, P. Ciais, G. Sampaio, B. Kruijt, P. Meir, P. Moorcroft, K. Zhang, E. Alvarez-Davila, A. A. de Oliveira, I. Amaral, A. Andrade, L. E. O. C. Aragao, A. Araujo-Murakami, E. J. M. M. Arets, L. Arroyo, G. A. Aymard, C. Baraloto, J. Barroso, D. Bonal, R. Boot, J. Camargo, J. Chave, A. Cogollo, F. C. Valverde, A. C. Lola da Costa, A. D. Fiore, L. Ferreira, N. Higuchi, E. N. Honorio, T. J. Killeen, S. G. Laurance, W. F. Laurance, J. Licona, T. Lovejoy, Y. Malhi, B. Marimon, B. H. M. Junior, D. C. L. Matos, C. Mendoza, D. A. Neill, G. Pardo, M. Pena-Claros, N. C. A. Pitman, L. Poorter, A. Prieto, H. Ramirez-Angulo, A. Roopsind, A. Rudas, R. P. Salomao, M. Silveira, J. Stropp, H. T. Steege, J. Terborgh, R. Thomas, M. Toledo, A. Torres-Lezama, G. M. F. van der Heijden, R. Vasquez, I. C. G. Vieira, E. Vilanova, V. A. Vos, T. R. Baker, Variation in stem mortality rates determines patterns of above-ground biomass in Amazonian forests: Implications for dynamic global vegetation models. *Glob. Chang. Biol.* **22**, 3996–4013 (2016).

33. D. Nepstad, P. Lefebvre, U. Lopes da Silva, J. Tomasella, P. Schlesinger, L. Solorzano, P. Moutinho, D. Ray, J. Guerreira Benito, Amazon drought and its implications for forest flammability and tree growth: A basin–wide analysis. *Glob. Chang. Biol.* **10**, 704–717 (2004).

34. A. C. Bennett, N. G. Mcdowell, C. D. Allen, K. J. Anderson-Teixeira, Larger trees suffer most during drought in forests worldwide. *Nat. Plants* **1**, 15139 (2015).

35. L. Rowland, A. C. L. da Costa, D. R. Galbraith, R. S. Oliveira, O. J. Binks, A. A. R. Oliveira, A. M. Pullen, C. E. Doughty, D. B. Metcalfe, S. S. Vasconcelos, L. V. Ferreira, Y. Malhi, J. Grace, M. Mencuccini, P. Meir, Death from drought in tropical forests is triggered by hydraulics not carbon starvation. *Nature* **528**, 119–122 (2015).

36. M. J. P. Sullivan, S. L. Lewis, K. Affum-Baffoe, C. Castilho, F. Costa, A. C. Sanchez, C. E. N. Ewango, W. Hubau, B. Marimon, A. Monteagudo-Mendoza, L. Qie, B. Sonke, R. V. Martinez, T. R. Baker, R. J. W. Brienen, T. R. Feldpausch, D. Galbraith, M. Gloor, Y. Malhi, S.-I. Aiba, M. N. Alexiades, E. C. Almeida, E. A. de Oliveira, E. A. Davila, P. A. Loayza, A. Andrade, S. A. Vieira, L. E. O. C. Aragao, A. Araujo-Murakami, E. J. M. M. Arets, L. Arroyo, P. Ashton, C. Gerardo Aymard, F. B. Baccaro, L. F. Banin, C. Baraloto, P. B. Camargo, J. Barlow, J. Barroso, J.-F. Bastin, S. A. Batterman, H. Beeckman, S. K. Begne, A. C. Bennett, E. Berenguer, N. Berry, L. Blanc, P. Boeckx, J. Bogaert, D. Bonal, F. Bongers, M. Bradford, F. Q. Brearley, T. Brncic, F. Brown, B. Burban, J. L. Camargo, W. Castro, C. Ceron, S. C. Ribeiro, V. C. Moscoso, J. Chave, E. Chezeaux, C. J. Clark, F. C. de Souza, M. Collins, J. A. Comiskey, F. C. Valverde, M. C. Medina, L. da Costa, M. Dančak, G. C. Dargie, S. Davies, N. D. Cardozo, T. de Haulleville, M. B. de Medeiros, J. D. A. Pasquel, G. Derroire, A. D. Fiore, J.-L. Doucet, A. Dourdain, V. Droissart, L. F. Duque, R. Ekoungoulou, F. Elias, T. Erwin, A. Esquivel-Muelbert, S. Fauset, J. Ferreira, G. F. Llampazo, E. Foli, A. Ford, M. Gilpin, J. S. Hall, K. C. Hamer, A. C. Hamilton, D. J. Harris, T. B. Hart, R. Hedl, B. Herault, R. Herrera, N. Higuchi, A. Hladik, E. H. Coronado, I. Huamantupa-Chuquimaco, W. H. Huasco, K. J. Jeffery, E. Jimenez-Rojas, M. Kalamandeen, M. N. K. Djuikouo, E. Kearsley, R. K. Umetsu, L. K. Kho, T. Killeen, K. Kitayama, B. Klitgaard, A. Koch, N. Labriere, W. Laurance, S. Laurance, M. E. Leal, A. Levesley, A. J. N. Lima, J. Lisingo, A. P. Lopes, G. Lopez-Gonzalez, T. Lovejoy, J. C. Lovett, R. Lowe, W. E. Magnusson, J. Malumbres-Olarte, A. G. Manzatto, B. H. Marimon Jr., A. R. Marshall, T. Marthews, S. M. de Almeida Reis, C. Maycock, K. Melgaco, C. Mendoza, F. Metali, V. Mihindou, W.

Milliken, E. T. A. Mitchard, P. S. Morandi, H. L. Mossman, L. Nagy, H. Nascimento, D. Neill, R. Nilus, P. N. Vargas, W. Palacios, N. P. Camacho, J. Peacock, C. Pendry, M. C. P. Mora, G. C. Pickavance, J. Pipoly, N. Pitman, M. Playfair, L. Poorter, J. R. Poulsen, A. D. Poulsen, R. Preziosi, A. Prieto, R. B. Primack, H. Ramirez-Angulo, J. Reitsma, M. Rejou-Mechain, Z. R. Correa, T. R. de Sousa, L. R. Bayona, A. Roopsind, A. Rudas, E. Rutishauser, K. A. Salim, R. P. Salomao, J. Schietti, D. Sheil, R. C. Silva, J. S. Espejo, C. S. Valeria, M. Silveira, M. Simo-Droissart, M. F. Simon, J. Singh, Y. C. S. Shareva, C. Stahl, J. Stropp, R. Sukri, T. Sunderland, M. Svatek, M. D. Swaine, V. Swamy, H. Taedoumg, J. Talbot, J. Taplin, D. Taylor, H. T. Steege, J. Terborgh, R. Thomas, S. C. Thomas, A. Torres-Lezama, P. Umunay, L. V. Gamarra, G. van der Heijden, P. van der Hout, P. van der Meer, M. van Nieuwstadt, H. Verbeeck, R. Vernimmen, A. Vicentini, I. C. G. Vieira, E. V. Torre, J. Vleminckx, V. Vos, O. Wang, L. J. T. White, S. Willcock, J. T. Woods, V. Wortel, K. Young, R. Zagt, L. Zemagho, P. A. Zuidema, J. A. Zwerts, O. L. Phillips, Long-term thermal sensitivity of earth's tropical forests. *Science* **368**, 869–874 (2020).

37. K. G. MacDicken, G. V. Wolf, C. B. Briscoe, *Standard Research Methods for Multipurpose Trees and Shrubs* (Winrock International, 1991).

38. J. Talbot, S. L. Lewis, G. Lopez-Gonzalez, R. J. W. Brienen, A. Monteagudo, T. R. Baker, T. R. Feldpausch, Y. Malhi, M. Vanderwel, A. Araujo Murakami, L. P. Arroyo, K.-J. Chao, T. Erwin, G. Van Der Heijden, H. Keeling, T. Killeen, D. Neill, P. N. Vargas, G. A. Parada Gutierrez, N. Pitman, C. A. Quesada, M. Silveira, J. Stropp, O. L. Phillips, Methods to estimate aboveground wood productivity from long-term forest inventory plots. *For. Ecol. Manage* **320**, 30–38 (2014).

39. Angiosperm Phylogeny Group, M. W. Chase, M. J. M. Christenhusz, M. F. Fay, J. W. Byng, W. S. Judd, D. E. Soltis, D. J. Mabberley, A. N. Sennikov, P. S. Soltis, P. F. Stevens, M. W. Chase, M. J. M. Christenhusz, M. F. Fay, J. W. Byng, W. S. Judd, D. E. Soltis, D. J. Mabberley, A. N. Sennikov, P. S. Soltis, P. F. Stevens, An update of the Angiosperm Phylogeny Group classification for the orders and families of flowering plants: APG IV. *Bot. J. Linn. Soc.* **181**, 1–20 (2016).

40. J. Chave, D. Coomes, S. Jansen, S. L. Lewis, N. G. Swenson, A. E. Zanne, Towards a worldwide wood economics spectrum. *Ecol. Lett.* **12**, 351–366 (2009).

41. J. Chave, M. Rejou-Mechain, A. Burquez, E. Chidumayo, M. S. Colgan, W. B. C. Delitti, A. Duque, T. Eid, P. M. Fearnside, R. C. Goodman, M. Henry, A. Martinez-Yrizar, W. A. Mugasha, H. C. Muller-Landau, M. Mencuccini, B. W. Nelson, A. Ngomanda, E. M. Nogueira, E. Ortiz-Malavassi, R. Pelissier, P. Ploton, C. M. Ryan, J. G. Saldarriaga, G. Vieilledent, Improved allometric models to estimate the aboveground biomass of tropical trees. *Glob. Chang. Biol.* **20**, 3177–3190 (2014).

42. M. Rejou-Mechain, A. Tanguy, C. Piponiot, J. Chave, B. Herault, biomass: An r package for estimating above-ground biomass and its uncertainty in tropical forests. *Methods Ecol. Evol.* **8**, 1163–1167 (2017).

43. E. V. S. B. Sampaio, G. C. Silva, Equacoes para estimar a biomassa de plantas da caatinga do semi-arido brasileiro. *Acta Bot. Bras.* **19**, 935–943 (2005).

44. A. R. Martin, M. Doraisami, S. C. Thomas, Global patterns in wood carbon concentration across the world's trees and forests. *Nat. Geosci.* **11**, 915–920 (2018).

45. I. Harris, T. J. Osborn, P. Jones, D. Lister, Version 4 of the CRU TS monthly high-resolution gridded multivariate climate dataset. *Sci. Data* **7**, 109 (2020).

46. S. E. Fick, R. J. Hijmans, WorldClim 2: New 1-km spatial resolution climate surfaces for global land areas. *Int. J. Climatol.* **37**, 4302–4315 (2017).

47. S. Peng, Y. Ding, W. Liu, Z. Li, 1 km monthly temperature and precipitation dataset for China from 1901 to 2017. *Earth Syst. Sci. Data* **11**, 1931–1946 (2019).

48. National Oceanic and Atmospheric Administration, Trends in atmospheric carbon dioxide (Earth System Research Laboratories, Global Monitoring Laboratory, 2020); www.esrl.noaa.gov/gmd/ccgg/trends/weekly.html.

49. EMBRAPA, *Manual De Métodos De Análise De Solos* (EMBRAPA/Centro Nacional de Pesquisa de Solos, ed. 2, 1997).

50. R Core Team, *R: A Language and Environment for Statistical Computing* (R Foundation for Statistical Computing, 2019); www.r-project.org/.

51. S. N. Wood, *Generalized Additive Models: An Introduction with R* (CRC Press, 2017).

52. D. Bates, M. Machler, B. Bolker, S. Walker, Fitting linear mixed-effects models using lme4. *J. Stat. Softw.* **67**, 1–48 (2015).

53. O. N. Bjornstad, *ncf: Spatial Covariance Functions. R package version 1.2-6* (2018); https://cran.r-project.org/package=ncf.

54. K. P. Burnham, D. R. Anderson, K. P. Huyvaert, AIC model selection and multimodel inference in behavioral ecology: Some background, observations, and comparisons. *Behav. Ecol. Sociobiol.* **65**, 23–35 (2011).

55. C. F. Dormann, J. Elith, S. Bacher, C. Buchmann, G. Carl, G. Carre, J. R. G. Marquez, B. Gruber, B. Lafourcade, P. J. Leitao, T. Munkemuller, C. McClean, P. E. Osborne, B. Reineking, B. Schroder, A. K. Skidmore, D. Zurell, S. Lautenbach, Collinearity: A review of methods to deal with it and a simulation study evaluating their performance. *Ecography* **36**, 27–46 (2013).

56. K. Barton, *MuMIn: Multi-Model Inference. R package version 1.42.1* (2018); https://cran.r-project.org/package=MuMIn.

57. S. Nakagawa, H. Schielzeth, A general and simple method for obtaining *R2* from generalized linear mixed-effects models. *Methods Ecol. Evol.* **4**, 133–142 (2013).

58. H. Wickham, *ggplot2: Elegant Graphics for Data Analysis* (Springer, 2016).

59. S. Garnier, *viridis: Default Color Maps from "matplotlib". R package version 0.5.1* (2018); https://cran.r-project.org/package=viridis.

60. T. Wei, V. Simko, *R package "corrplot": Visualization of a Correlation Matrix (Version 0.84)* (2017); https://github.com/taiyun/corrplot.

61. A. Liaw, M. Wiener, Classification and regression by randomforest. *R News* **2**, 18–22 (2002).

Acknowledgments: We thank the Federal University of Lavras (UFLA) and all students who collected the data used in this study over time. **Funding:** This study was funded by the State of Minas Gerais Research Foundation (FAPEMIG), the National Council for Scientific and Technological Development (CNPq), and the Coordination for the Improvement of Higher Education Personnel (CAPES). **Author contributions:** V.A.M. and R.M.d.S. conceived the ideas and designed methodology. A.B.M.S., C.R.d.S., T.A.V., L.C.A.d.S., R.T.P., N.C.A.F., G.G.P.d.P., P.A.C., P.O.G., M.A.L.F., F.M.G., F.d.O., D.T.G., J.D.M., P.F.S., F.d.C.A., N.d.A.-C., C.L.F., G.C.d.O.M., M.A.L.F., W.B.d.S., R.M.d.S., and V.A.M. collected the data. V.A.M. analyzed the data. V.A.M., A.B.M.S., and N.d.A.-C. led the writing of the manuscript. C.L.F. and C.R.d.S. curated the data. P.A.C., N.d.A.-C., M.C.F.d.O., L.C.A.d.S., and J.D.M. edited the manuscript. All authors contributed critically to the drafts and gave final approval for publication. **Competing interests:** The authors declare that they have no competing interests. **Data and materials availability:** Forest inventory raw data are hosted in the ForestPlots.net system and bound to data-use restrictions defined on Forestplots.net (www.forestplots.net) (see area codes in table S1). All data needed to evaluate the conclusions in the paper are present in the Supplementary Materials (data files S1 and S2). The R codes are available upon request from the corresponding author.

Submitted 22 June 2020
Accepted 30 October 2020
Published 18 December 2020
10.1126/sciadv.abd4548

Citation: V. A. Maia, A. B. M. Santos, N. de Aguiar-Campos, C. R. de Souza, M. C. F. de Oliveira, P. A. Coelho, J. D. Morel, L. S. da Costa, C. L. Farrapo, N. C. A. Fagundes, G. G. P. de Paula, P. F. Santos, F. M. Gianasi, W. B. da Silva, F. de Oliveira, D. T. Girardelli, F. de Carvalho Araujo, T. A. Vilela, R. T. Pereira, L. C. A. da Silva, G. C. de Oliveira Menino, P. O. Garcia, M. A. L. Fontes, R. M. dos Santos, The carbon sink of tropical seasonal forests in southeastern Brazil can be under threat. *Sci. Adv.* **6**, eabd4548 (2020).

SUPPLEMENTARY MATERIALS

The carbon sink of tropical seasonal forests in southeastern Brazil can be under threat

Vinícius Andrade Maia[1]*, Alisson Borges Miranda Santos[1,] Natália de Aguiar-Campos[1], Cléber Rodrigo de Souza[1], Matheus Coutinho Freitas de Oliveira[1], Polyanne Aparecida Coelho[1], Jean Daniel Morel[1], Lauana Silva da Costa[1], Camila Laís Farrapo[1], Nathalle Cristine Alencar Fagundes[1,2,3], Gabriela Gomes Pires de Paula[1], Paola Ferreira Santos[2], Fernanda Moreira Gianasi[2], Wilder Bento da Silva[1], Fernanda de Oliveira[2], Diego Teixeira Girardelli[1], Felipe de Carvalho Araújo[1, 2], Taynara Andrade Vilela[1], Rafaella Tavares Pereira[1], Lidiany Carolina Arantes da Silva[1], Gisele Cristina de Oliveira Menino[4], Paulo Oswaldo Garcia[5], Marco Aurélio Leite Fontes[1], Rubens Manoel dos Santos[1,2]*.

Correspondence to: vinicius.a.maia77@gmail.com, rubensmanoel@ufla.br

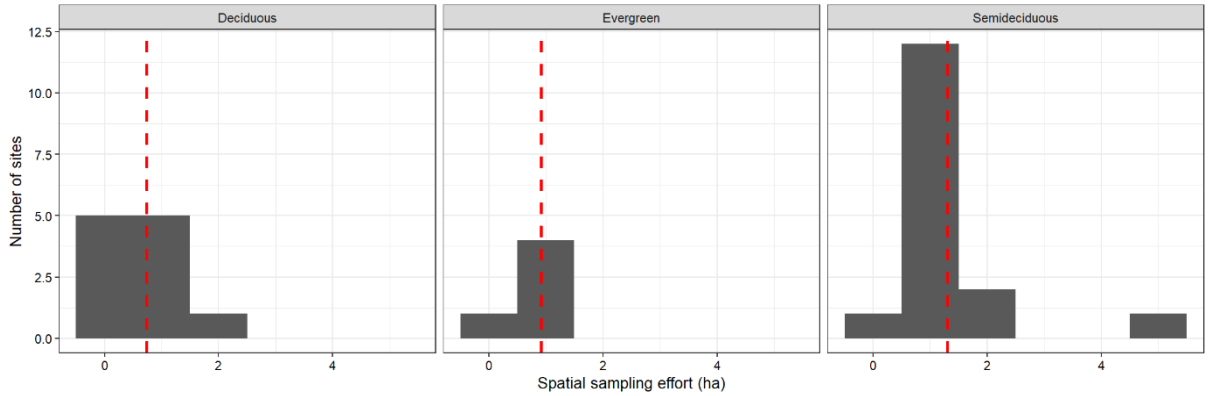

Fig. S1. **Frequency of site sampled area by forest type.** The red dashed line is the mean of the sampled area among sites by forest type (n = 32). Deciduous forests (n = 11) (mean 0.73 ha), evergreen forests (n = 5) (mean 0.92 ha), semideciduous forests (n = 16) (mean 1.3 ha).

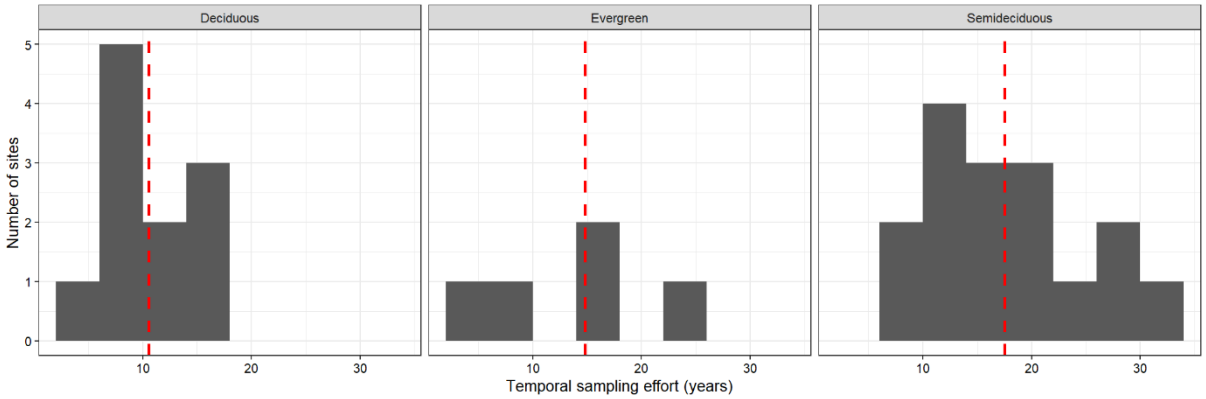

Fig. S2. **Frequency of site total monitoring length by forest type.** The site total monitoring length is calculated as the year of the last census minus the year of first census, the red dashed line is the mean of the total monitoring length among sites by forest type (n = 32). Deciduous forests (n = 11) (mean 10.5 years), evergreen forests (n = 5) (mean 14.8 years), semideciduous forests (n = 16) (mean = 17.5 years).

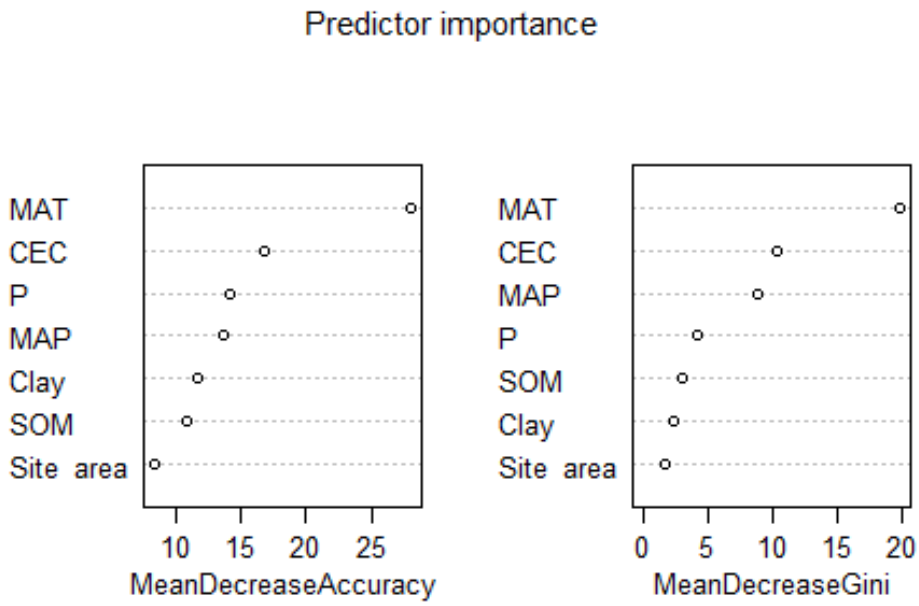

Fig. S3. **Climate, soil and site area importance for predicting forest type.** The importances (mean decrease in accuracy and mean decrease in Gini index) were estimated using random forest (*61*) algorithm with forest type as function of climate, soil and site area. Note that only the variables included in the global model (after drop collinear variables) were included in the random forest.

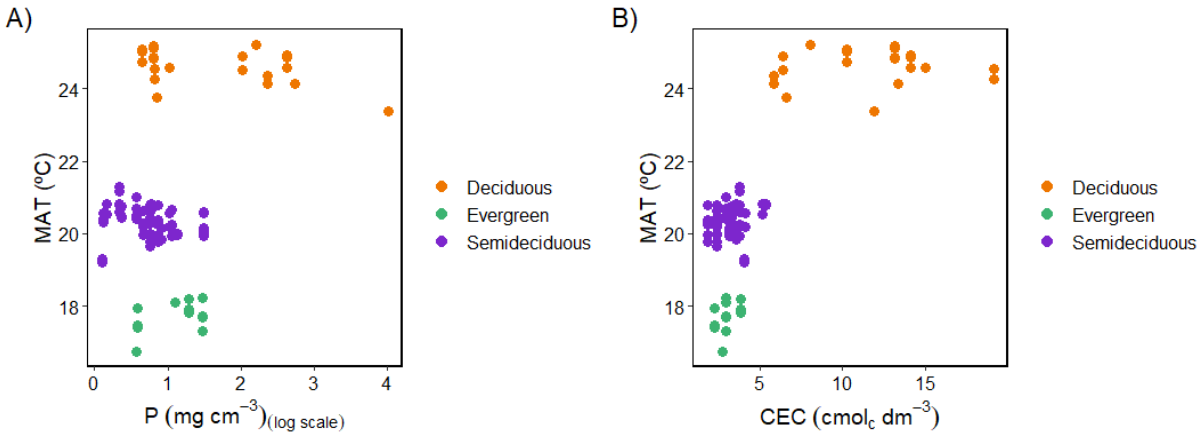

Fig. S4. **Distribution of the sites and forest types over the environmental space.** The environmental space is represented by mean annual temperature (MAT) and **(A)** soil phosphorus (P) (log scale to ease visualization), **(B)** cation exchange capacity (CEC). Data with census intervals (n = 95) nested within sites.

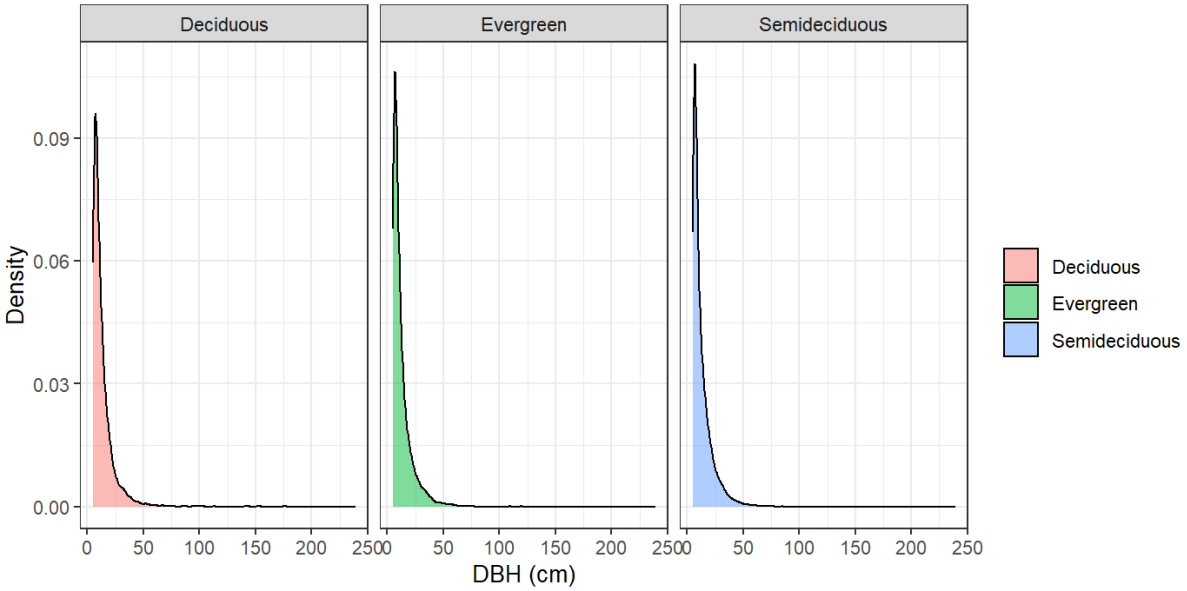

Fig. S5. Kernel density estimate of quadratic diameter at breast height (DBH) by forest type. (n = 201,415).

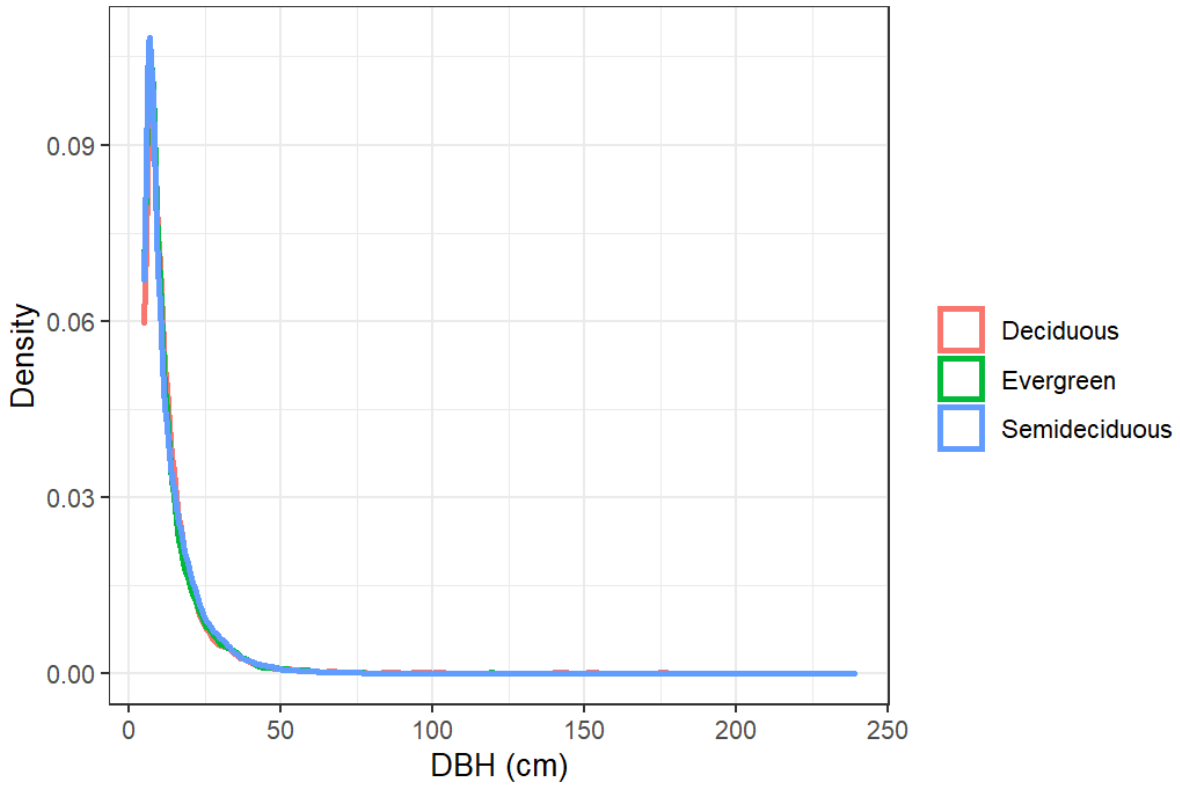

Fig. S6. **Kernel density estimate of quadratic diameter at breast height (DBH) by forest type.** (n = 201,415).

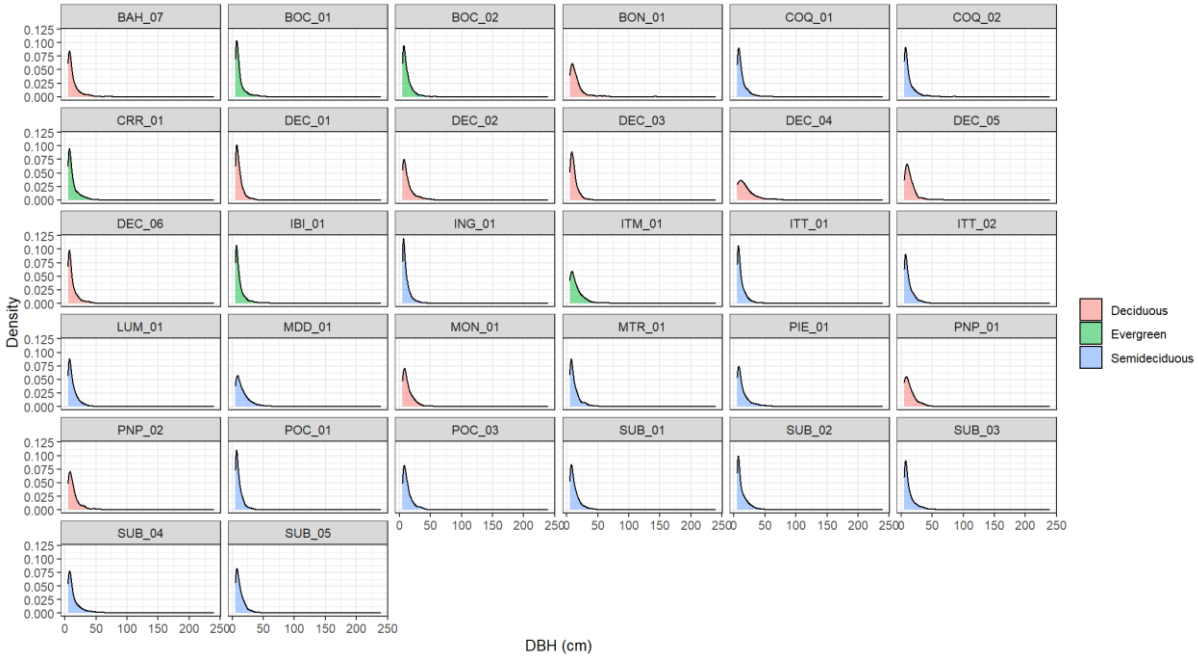

Fig. S7. **Kernel density estimate of quadratic diameter at breast height (DBH) by site.** The sites are colored accordingly to its forest type. (n = 201,415).

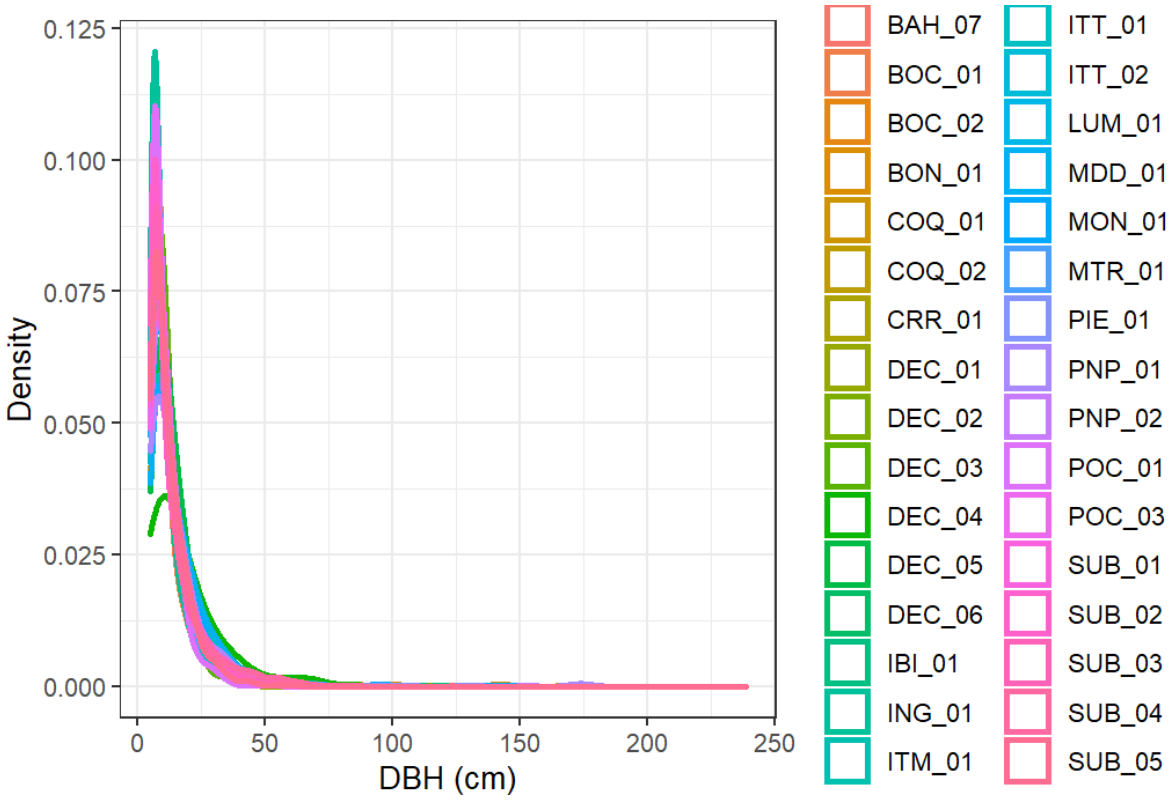

Fig. S8. Kernel density estimate of quadratic diameter at breast height (DBH) by site. (n = 201,415).

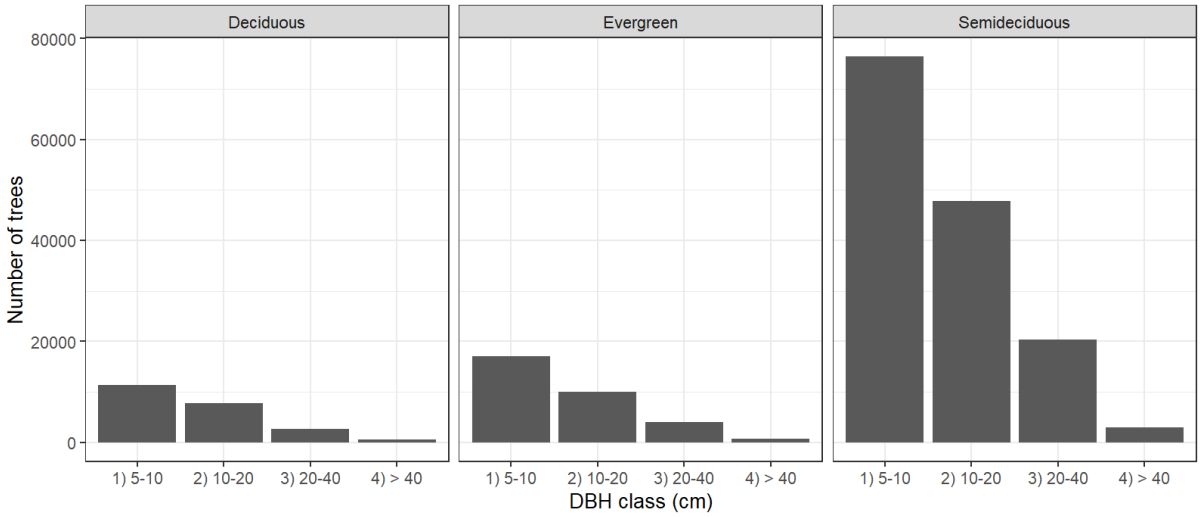

Fig. S9. **Number of trees within each DBH class by forest type.** (n = 201,415).

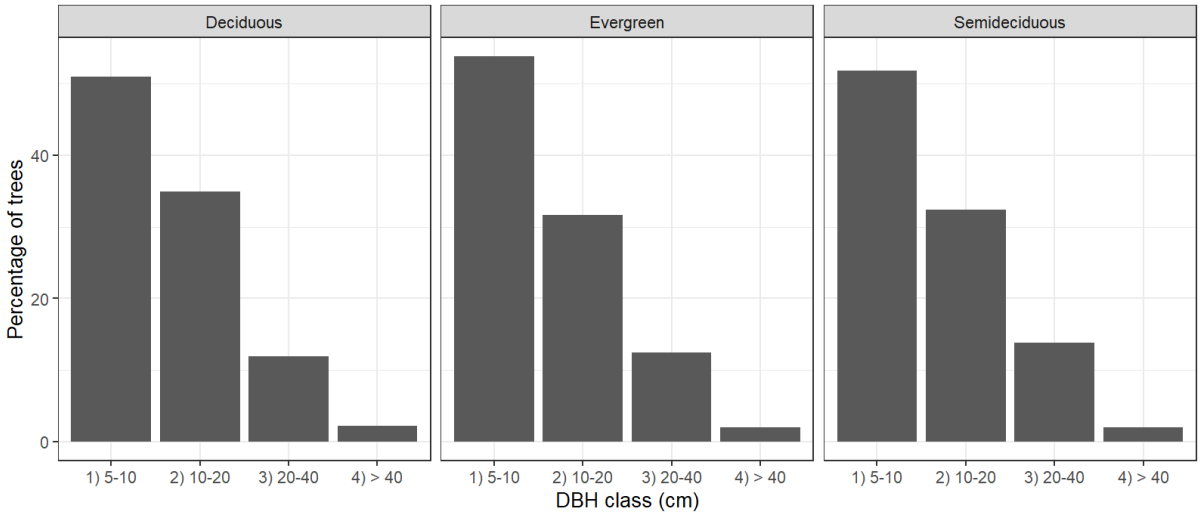

Fig. S10. **Percentage of trees within each DBH class by forest type.** The percentage was calculated by the ratio between the number of trees within a given DBH class and the total number of trees of the forest type. (n = 201,415).

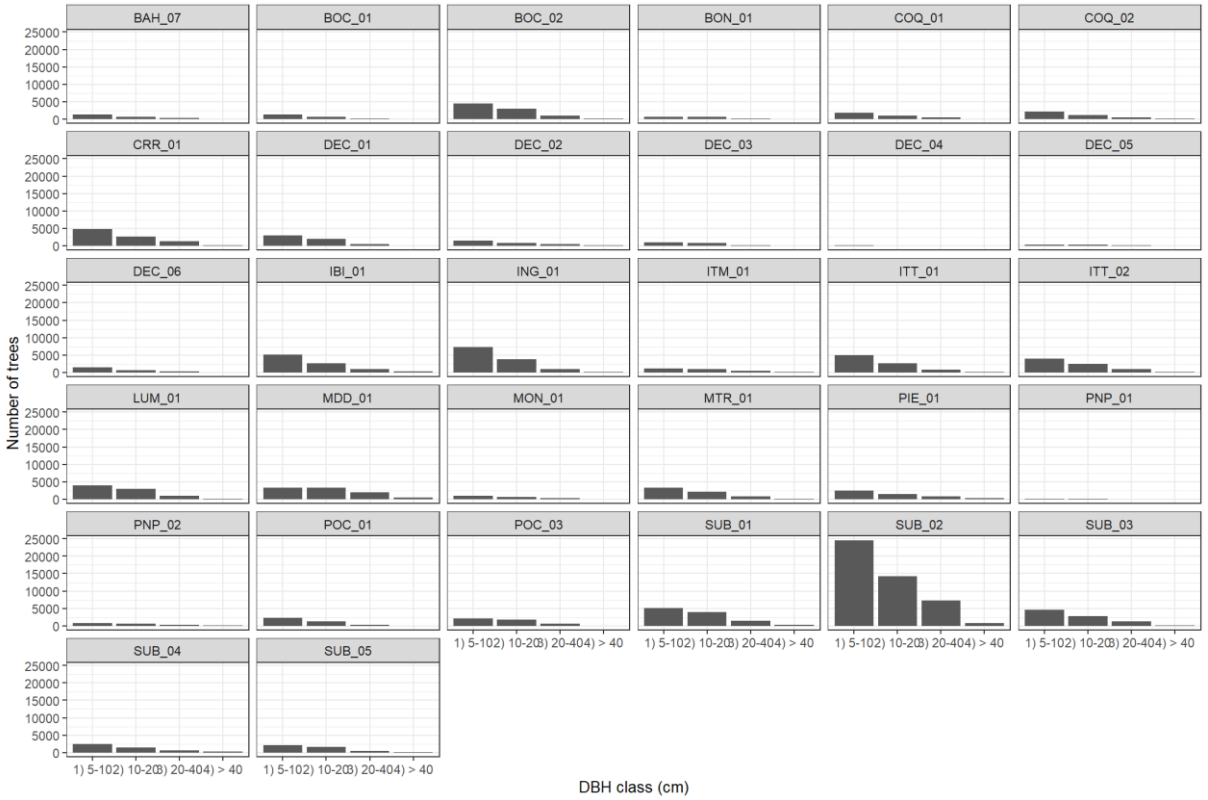

Fig. S11. **Number of trees within each DBH class by site.** (n = 201,415).

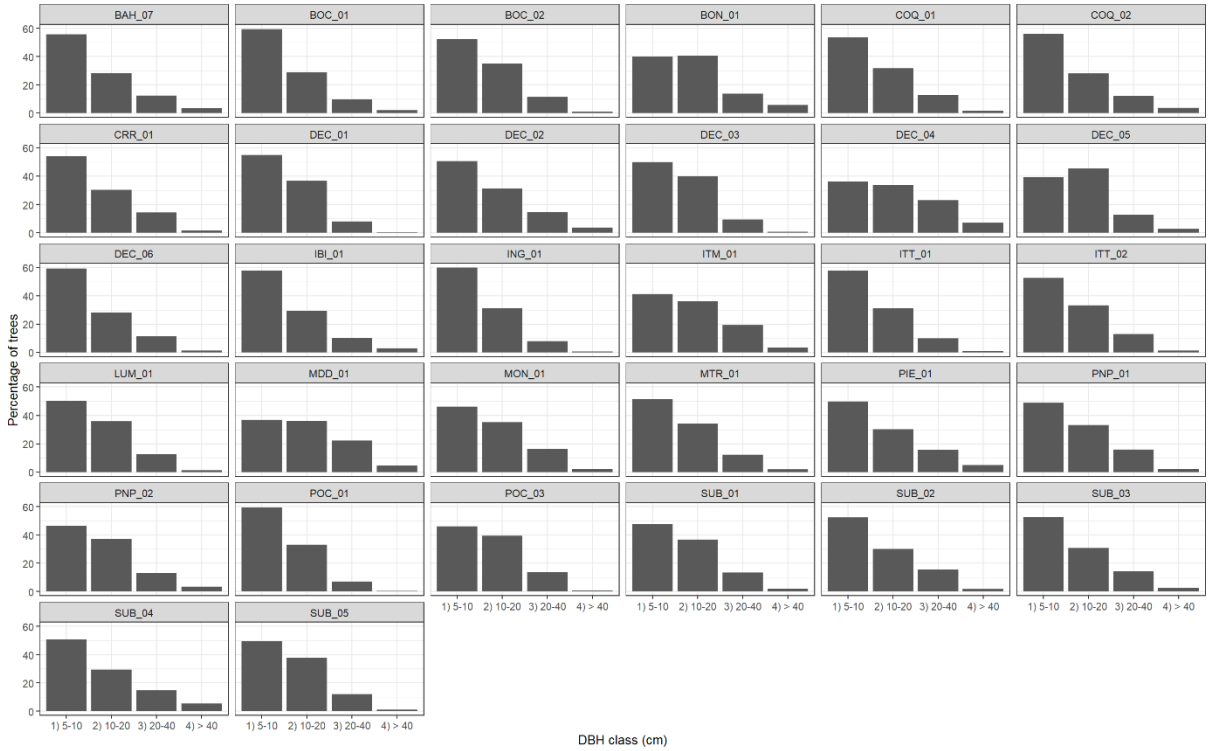

Fig. S12. **Percentage of trees within each DBH class by site.** The percentage was calculated by the ratio between the number of trees within a given DBH class and the total number of trees of the site. (n = 201,415).

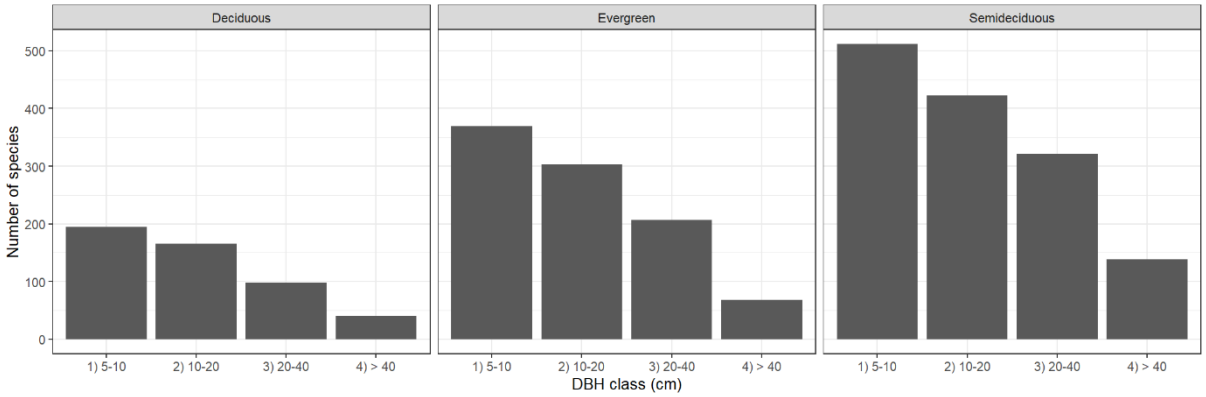

Fig. S13. **Number of tree species within each DBH class by forest type.** (n = 201,415).

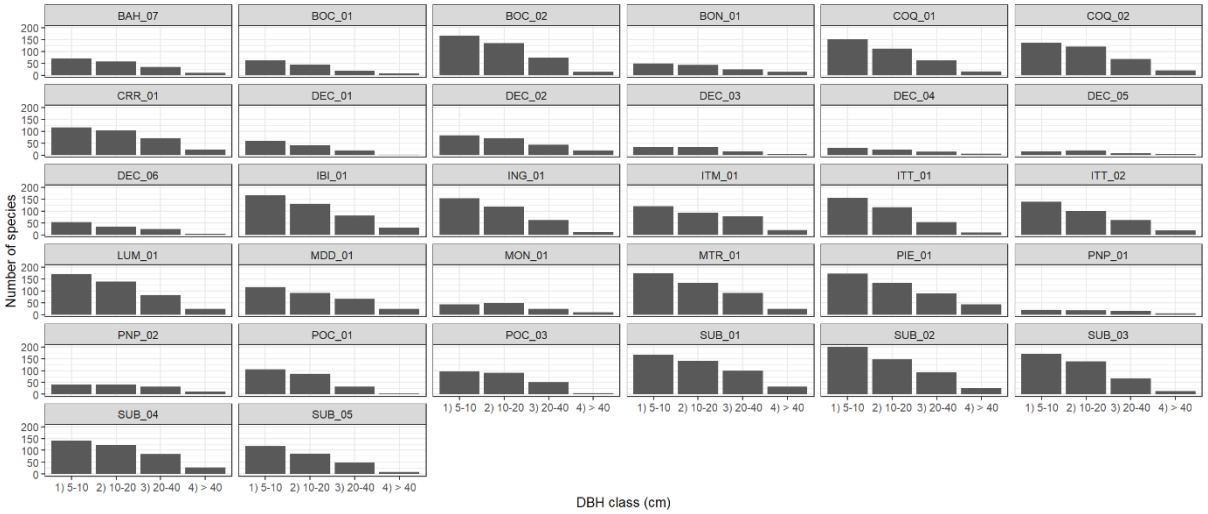

Fig. S14. **Number of tree species within each DBH class by site.** (n = 201,415).

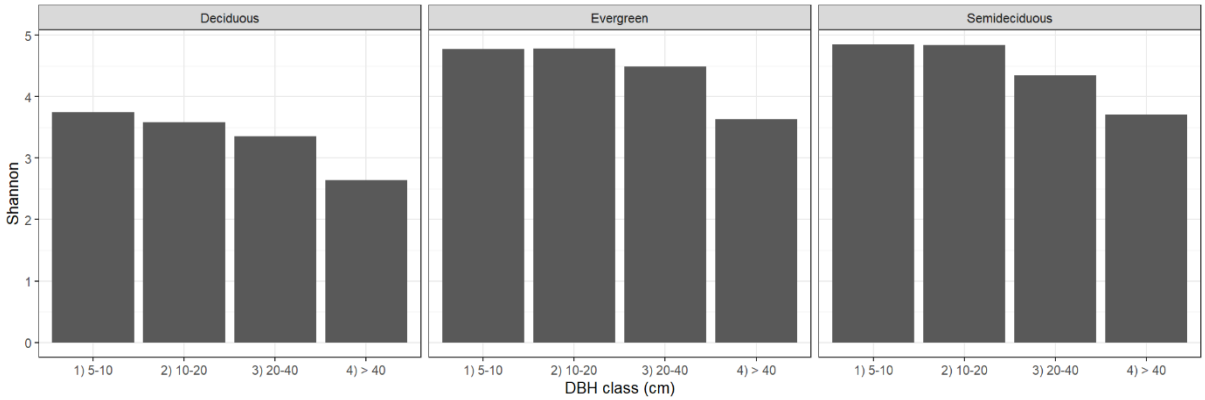

Fig. S15. **Shannon diversity index within each DBH class by forest type.** (n = 201,415).

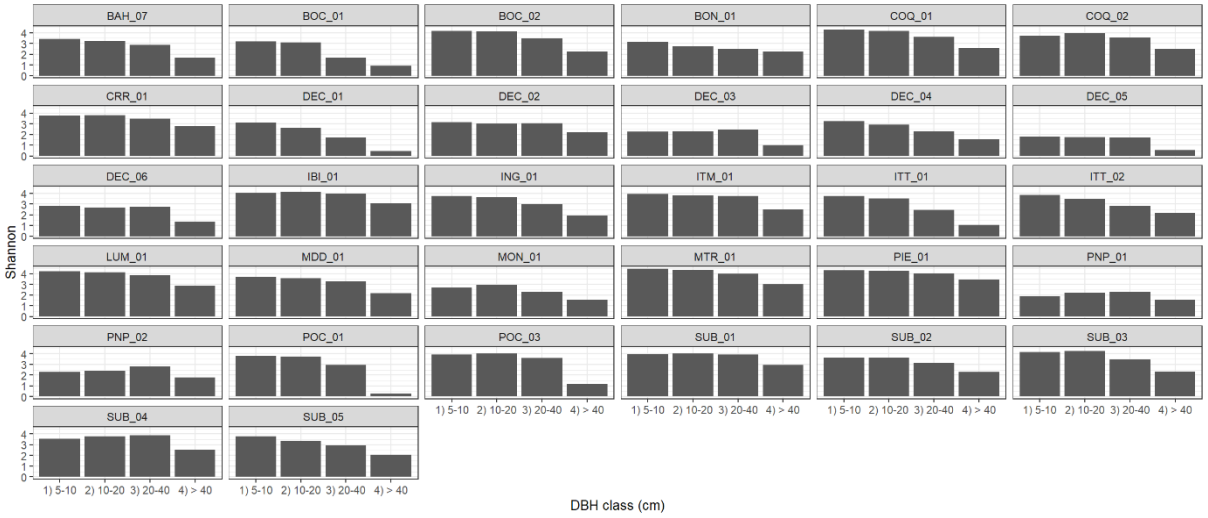

Fig. S16. **Shannon diversity index within each DBH class by site.** (n = 201,415).

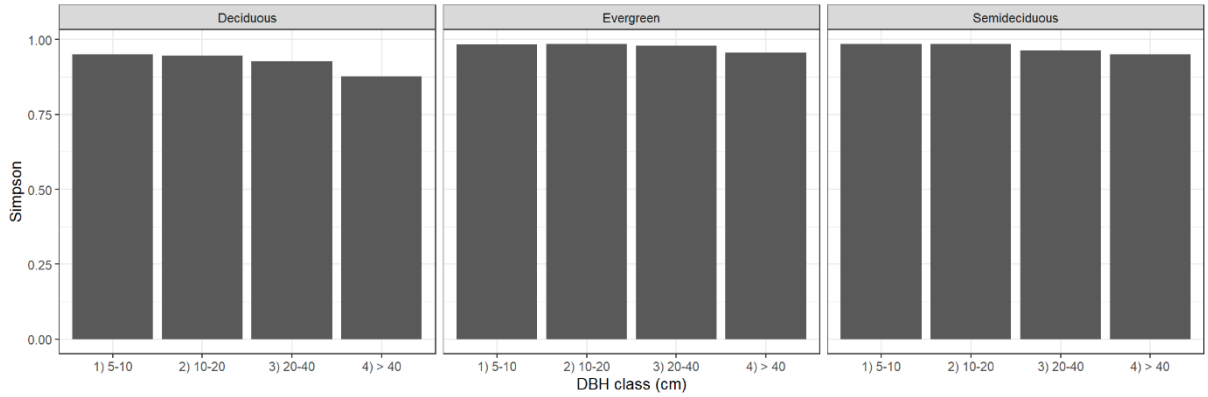

Fig. S17. **Simpson diversity index within each DBH class by forest type.** (n = 201,415).

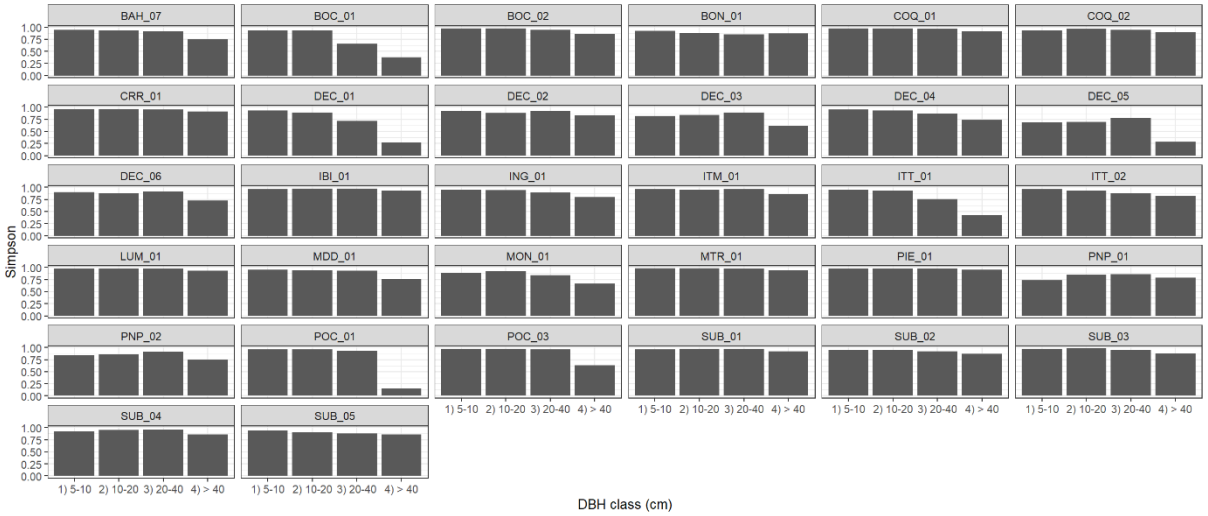

Fig. S18. **Simpson diversity index within each DBH class by site.** (n = 201,415).

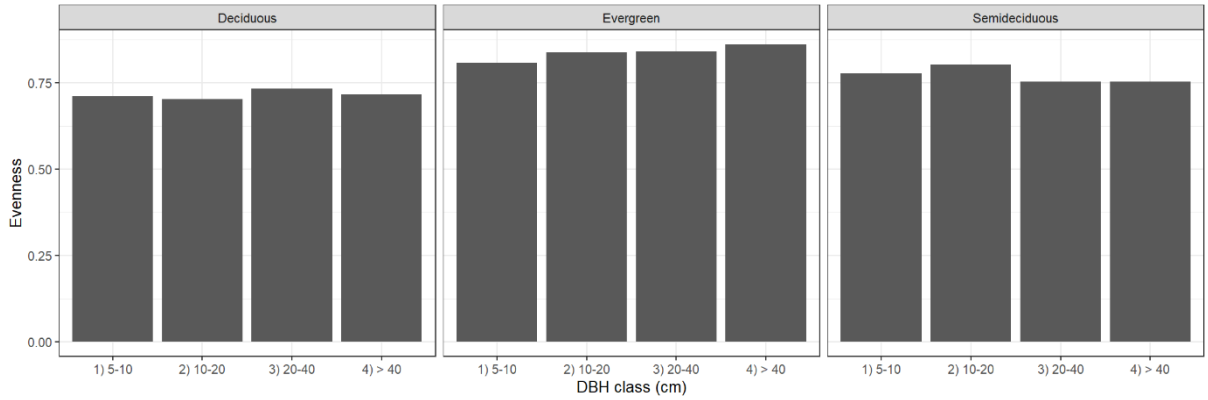

Fig. S19. **Pielou's evenness diversity index within each DBH class by forest type.** (n = 201,415).

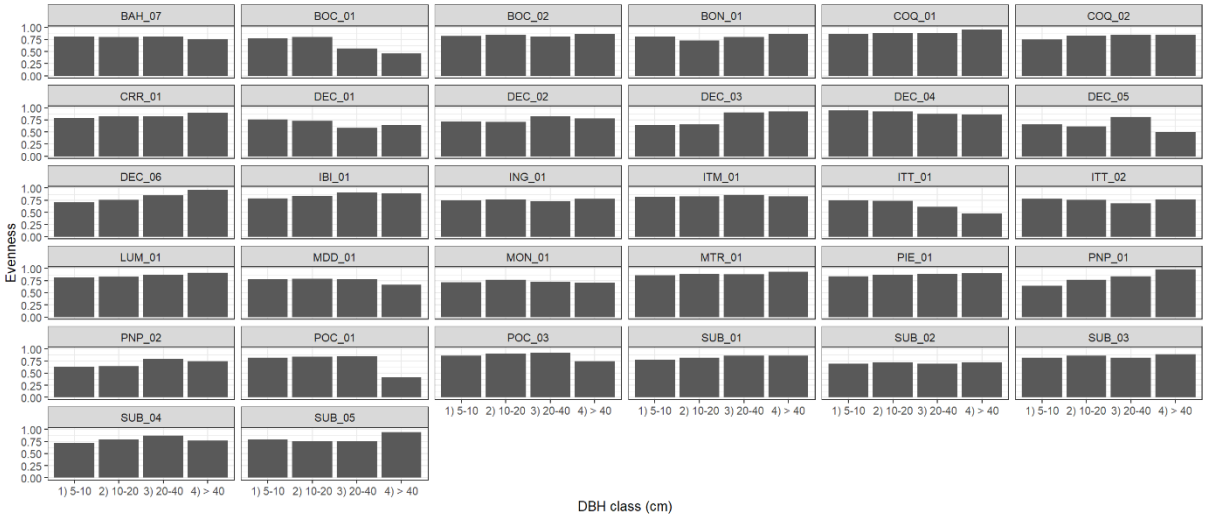

Fig. S20. Pielou's evenness diversity index within each DBH class by site. (n = 201,415).

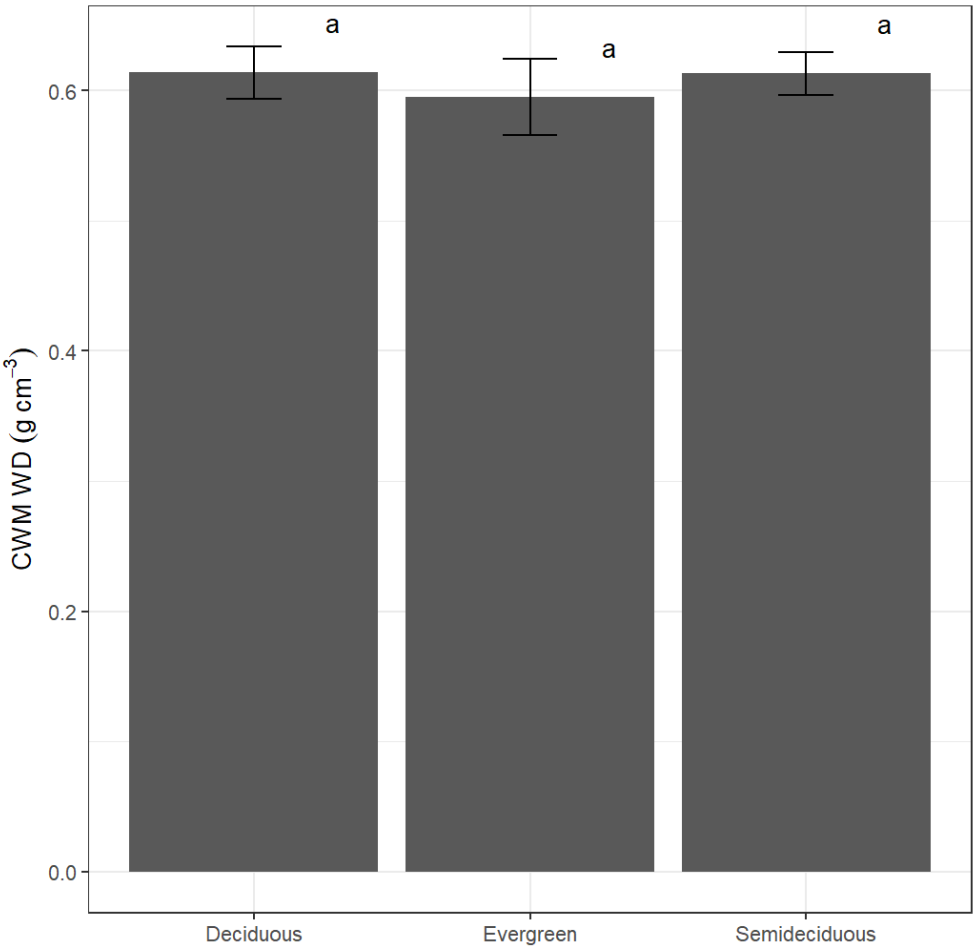

Fig. S21. Variation in wood density community weighted (by abundance) mean (CWM) among forest types. The means and confidence intervals were estimated with the estimated marginal means from linear mixed effects models (LMM, accounting for the random effect of site). Data with censuses (n = 127) nested within sites (n = 32).

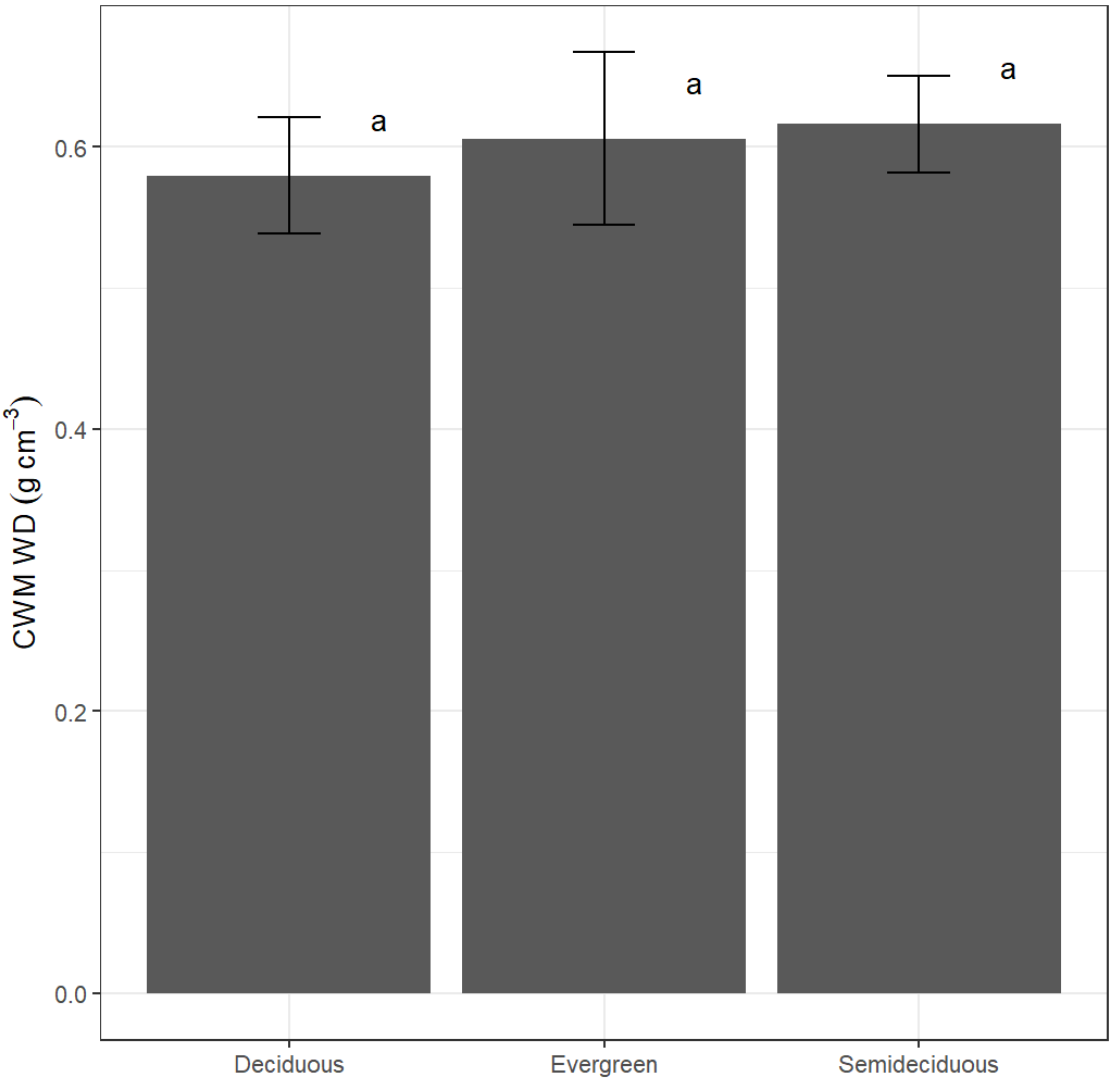

Fig. S22. **Variation in wood density community weighted (by aboveground woody biomass) mean (CWM) among forest types.** The means and confidence intervals were estimated with the estimated marginal means from linear mixed effects models (LMM, accounting for the random effect of site). Data with censuses (n = 127) nested within sites (n = 32).

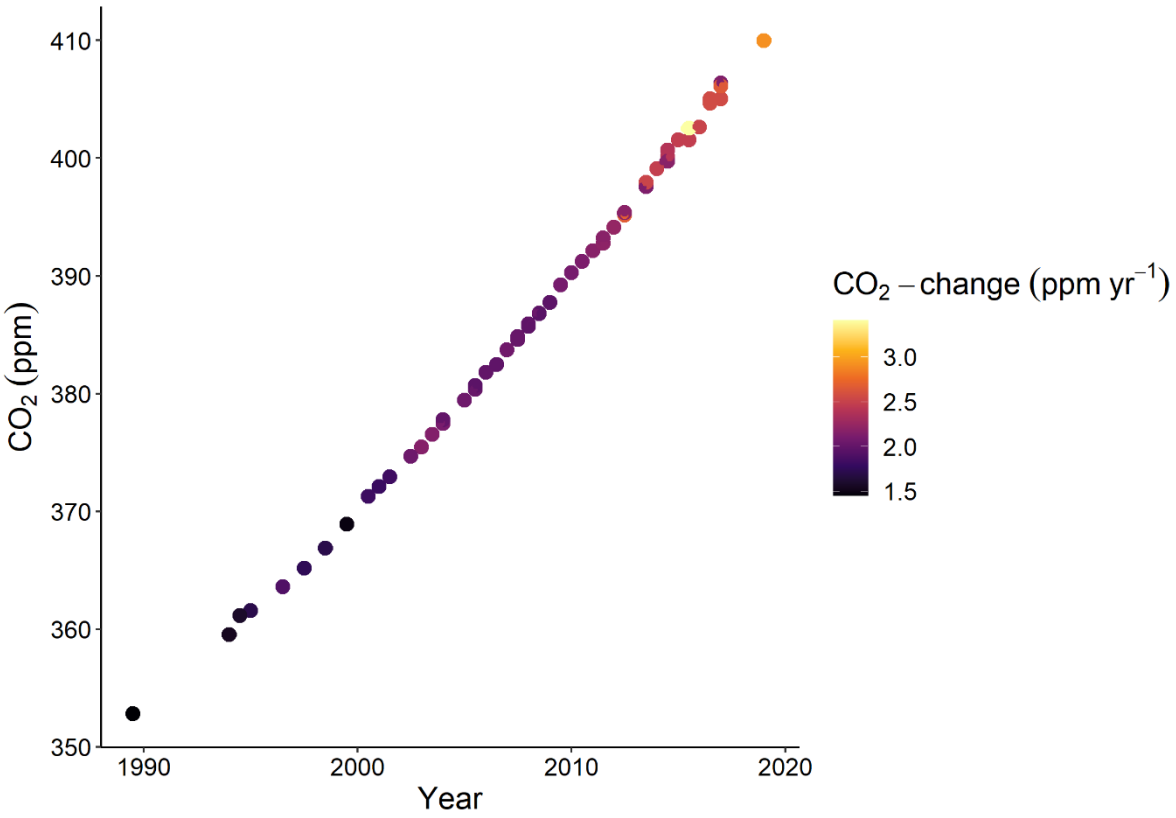

Fig. S23. **Relationship between atmospheric CO_2 concentration and time.** The points are colored accordingly CO_2-change. Data with census intervals (n = 95) nested within sites (n = 32).

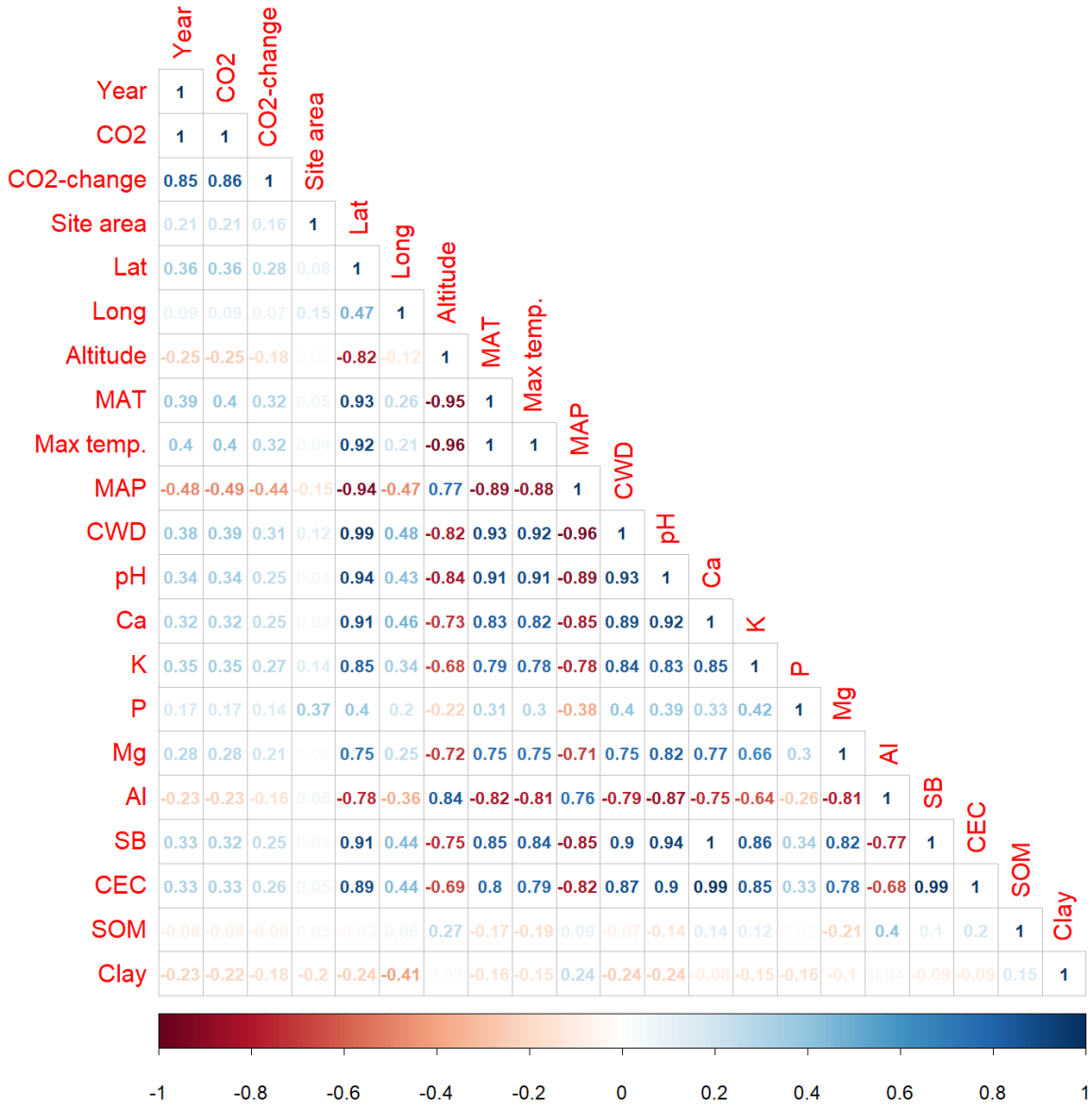

Fig. S24. Correlation matrix between potential predictors. Note: Year (Year), CO2 (CO_2 concentration), CO2-change (CO_2-change), Site area (Site area), Altitude, MAT (mean annual temperature), Max temp. (mean maximum temperature), MAP (mean annual precipitation), CWD (maximum climatological water deficit), pH (pH), Ca (calcium), K (potassium), P (phosphorus), Mg (Magnesium), Al (Aluminum), SB (sum of bases), CEC (cation exchange capacity), SOM (soil organic matter), Clay (clay %). Data with census intervals (n = 95) nested within sites (n = 32).

Table S1. This table shows each site (n = 32) (ForestPlots area code), with their latitude (Lat), longitude (Long), forest type, sampled area, number of censuses (N census), year of the first census (Year-start), year of the last census (Year-end), mean interval length among census intervals (Mean interval length), site area, mean of mean annual temperature among census intervals (MAT) and mean of mean annual precipitation among census intervals (MAP).

Site code	Lat	Long	Forest type	Sampled area (ha)	N census	Year-start	Year-end	Mean interval length (yr)	Site area (ha)	MAT (°C)	MAP (mm)
BAH_07	-14.4705	-44.1884	Deciduous	2.04	2	2002	2009	7	25	24.1	907.7
BOC_01	-22.1617	-44.4658	Evergreen	0.4	2	2004	2010	6	3	18.1	1739.4
BOC_02	-22.2175	-44.5389	Evergreen	1.04	4	2001	2019	6	20	17.6	1636.7
BON_01	-15.3116	-44.7349	Deciduous	0.6	3	2011	2018	3.5	17	24.2	868.3
COQ_01	-21.0946	-45.3482	Semideciduous	0.8	3	2007	2019	6	59	20.4	1565.9
COQ_02	-21.1553	-45.4714	Semideciduous	1	3	2002	2014	6	10	20.8	1559
CRR_01	-21.6121	-44.612	Evergreen	1.2	4	2001	2019	6	36	18	1795.7
DEC_01	-14.4138	-44.1627	Deciduous	0.8	5	2005	2020	3.8	50	25	747.6
DEC_02	-15.5502	-44.701	Deciduous	1.2	3	2007	2020	6.5	64	24.7	829.7
DEC_03	-14.5447	-44.2105	Deciduous	0.4	4	2005	2018	4.3	60	24.3	802.4
DEC_04	-14.2663	-44.1068	Deciduous	0.2	2	2005	2010	5	20	25.2	866.4
DEC_05	-14.4315	-44.4911	Deciduous	0.2	5	2005	2020	3.8	4	24.7	840.1
DEC_06	-14.4919	-44.1841	Deciduous	0.48	5	2005	2020	3.8	80	24.9	759.3
IBI_01	-21.7103	-43.8855	Evergreen	0.96	5	1995	2020	6.3	68	17.7	1621.6
ING_01	-21.4098	-44.8929	Semideciduous	1	5	1999	2018	4.8	17	20.7	1586
ITM_01	-22.3501	-44.7946	Evergreen	1	2	2011	2018	7	7	16.7	1613.6
ITT_01	-21.3526	-44.609	Semideciduous	0.945	5	1992	2019	6.8	4	20.3	1640.9
ITT_02	-21.3556	-44.6155	Semideciduous	0.84	5	1994	2019	6.3	9	20.3	1642.5
LUM_01	-21.4977	-44.9134	Semideciduous	1.28	4	2000	2019	6.3	77	20.6	1592.8
MDD_01	-21.4885	-44.3762	Semideciduous	1.53	7	1991	2019	4.7	20	20.2	1538.2
MON_01	-14.4401	-44.4246	Deciduous	1	2	2011	2020	9	40	24.6	782.8
MTR_01	-21.6069	-44.5569	Semideciduous	1.2	3	2010	2018	4	1200	20	1528.7
PIE_01	-21.4884	-44.1006	Semideciduous	1.2	3	1999	2010	5.5	30	19.3	1609.9
PNP_01	-15.1208	-44.2273	Deciduous	0.2	2	2011	2020	9	1000	23.4	731.7
PNP_02	-15.0583	-44.2069	Deciduous	0.96	2	2012	2020	8	800	23.7	691.7
POC_01	-21.3292	-44.9717	Semideciduous	0.78	3	2000	2011	5.5	90	20	1720.2
POC_03	-21.3292	-44.9717	Semideciduous	0.42	8	2001	2016	2.1	90	20.2	1572.2
SUB_01	-21.2214	-44.9631	Semideciduous	1.92	4	2001	2016	5	12	20.4	1650.8
SUB_02	-21.2278	-44.9639	Semideciduous	5.04	8	1987	2018	4.4	6	20.2	1609.2
SUB_03	-21.2737	-44.882	Semideciduous	1.12	6	1998	2020	4.4	11	20.9	1550.8
SUB_04	-21.2167	-44.9803	Semideciduous	1.16	4	2000	2017	5.7	4	20.6	1617.1
SUB_05	-21.15	-44.9	Semideciduous	0.6	4	2003	2011	2.7	59	20.7	1760.9